

Monte Carlo simulation applied to gamma-ray spectrometry

Octavian Sima

University of Bucharest, Romania

National Institute for Physics and Nuclear Engineering

“Horia Hulubei”

Bucharest-Magurele, Romania

Overview

1. Introduction
2. Simulation of the full energy peak efficiency
3. Efficiency transfer from the reference to the actual measurement
4. Special applications
 - Non-uniform activity distribution in the source
 - ^{226}Ra solution in the PTB ampoule
 - ^{60}Co and ^{134}Cs point sources with unknown position in a bulk sample
 - Compton suppressed spectrometers
 - Dead layer problem
5. Conclusions

1. Introduction

Direct experimental calibration possible or convenient only in specific cases:

- Point-like sources, volume sources with particular matrices
- Only for a limited number of nuclides (important when coincidence summing effects are significant)

⇒ Experimental calibration insufficient for current gamma-ray spectrometry:

- Broad range of applications (type, samples, nuclides – summing effects)
- High efficiency detectors, special applications
- Performance criteria (uncertainty, low detection limit)

⇒ Need for computational methods

- Analytical and semi-empirical methods – fast, but simplified models (certain features are approximated or neglected)
- Monte Carlo (MC) simulation
 - Realistic – can incorporate every physical process, accurate description of the source-detector geometry
 - Flexible
 - Computing time no longer a problem
 - Computer codes and computing power currently available

Present day applications:

- More refined solutions for the old problems:
 - *Precise efficiency calibration*
 - *Coincidence summing effects*
- More complex problems:
 - *Compton-suppressed spectrometers*
 - *Big volume samples*
 - *In situ measurements*
 - *Waste drums*
 - *Non-homogeneous sources (activity distribution, matrix)*

Simulation codes:

- More realistic description of the relevant physics processes
- Improved model of the detector
 - Inclusion of charge collection?
- Improved nuclear decay data
- Uncertainty estimation

=> The application of Monte Carlo simulation will be extended in the future

- Best approach to calibration:
 - Experimental calibration for a reference measurement
 - Correction factors by Monte Carlo

Most accurate efficiency calibration:

R.G. Helmer et al., NIMA 511 (2003) 360

- Combination of experimental calibration and MC simulation
- 70% n-type detector, point source at 15 cm from detector
- Relative efficiencies measured with sources which emit two or more photons with high and precisely known emission probabilities (^{48}Cr , ^{60}Co , ^{88}Y , $^{108\text{m}}\text{Ag}$, ^{109}Cd , $^{120\text{m}}\text{Sb}$, ^{133}Ba , ^{134}Cs , ^{137}Cs , $^{180\text{m}}\text{Hf}$)
- Absolute efficiency at 1173 and 1332 keV measured with a ^{60}Co source with activity uncertainty 0.06 % (95 % confidence level) - E. Schönfeld et al., ARI 56 (2002) 215
- Detector parameters: radiography + scanning
- Dead layer - low energy efficiency (with special care for Ge X-rays escape)

Results: most accurate efficiency calibration curve

- Uncertainty of the efficiency calibration:
 - 0.2 % from 50 keV to 1400 keV
 - 0.4 % from 1400 keV to 3500 keV

Today many Monte Carlo computer codes are available for application in gamma-ray spectrometry:

- *General simulation codes:*

- Advantages: realistic description of physics processes, well tested
- Disadvantage: computing time, may require user intervention
- Examples:
 - GEANT 4 (GEANT3.21)
 - PENELOPE
 - MCNP, MCNPX
 - EGS (EGS4, EGSnrc)
 - ITS - CYLTRAN
 - ETRAN ...

- *Specific purpose simulation codes:*

- Advantages: optimized for the particular problem, user friendly, faster
- Disadvantage: sometimes limited validity
- Examples (alphabetical order):
 - DETEFF
 - EFFTRAN
 - GESPECOR ...

Typical applications of Monte Carlo simulation in gamma-ray spectrometry (O. Sima, Encyclopedia of Analytical Chemistry, online, Wiley, 2012):

- Full energy peak efficiency
- Self-attenuation corrections
- Efficiency transfer from a reference geometry to a different geometry
- Coincidence-summing corrections

In what follows focus mainly on non-standard applications

2. Simulation of the full energy peak efficiency

Basically two types of computations:

- (a) Evaluation of the photon histories in which the complete energy was absorbed in the sensitive volume of the detector, without the simulation of the full spectrum
 - Usually applied in specific purpose codes
 - Fast computation – variance reduction techniques e.g. focalized emission towards the detector, analytical factor for attenuation between the emission point and the detector, forced first interaction in detector

- (b) Simulation of the spectrum and spectrum analysis
 - Usually when general purpose codes are applied (GEANT, PENELOPE, MCNP, EGS)
 - Analogue simulation, longer computing time

Simulation of the spectrum can result in the construction of:

(b1) Ideal spectrum, neglecting experimental resolution

- Disadvantage: Sensitivity of the calculation to the channel width (Vidmar et al., ARI 66 (2008) 764)
 - Large width: impossibility to discriminate the signals corresponding to photons that have lost a small fraction of energy outside the sensitive volume
 - Too narrow channel width: problems due to rounding errors

(b2) Realistic spectrum, including experimental resolution (Decombaz et al., NIM 312 (1992) 152)

- Advantage: The simulated spectrum can be analyzed with the same software as the experimental spectrum
 - The possible bias due to differences in spectrum analysis (e.g. definition of the efficiency, of the peak area) between experimental and simulated spectrum removed

Simulation can be applied also for sensitivity studies and for optimization of the measurement geometry

Input data required:

- Detector dimensions and mounting
- Source geometry, matrix

Caution:

- Is the detector model perfectly adequate? Uncertainties in detector dimensions, thickness of the dead layer?
- Problems with charge collection?
 - ⇒ Significant effect on the full energy peak efficiency
 - ⇒ Uncertainty of the efficiency

Parameter optimization

- X-ray radiography
- Scan with collimated photon beams
- Adjustment of parameters by trial-and-error
- Validation of the model

In the case of specific purpose programs

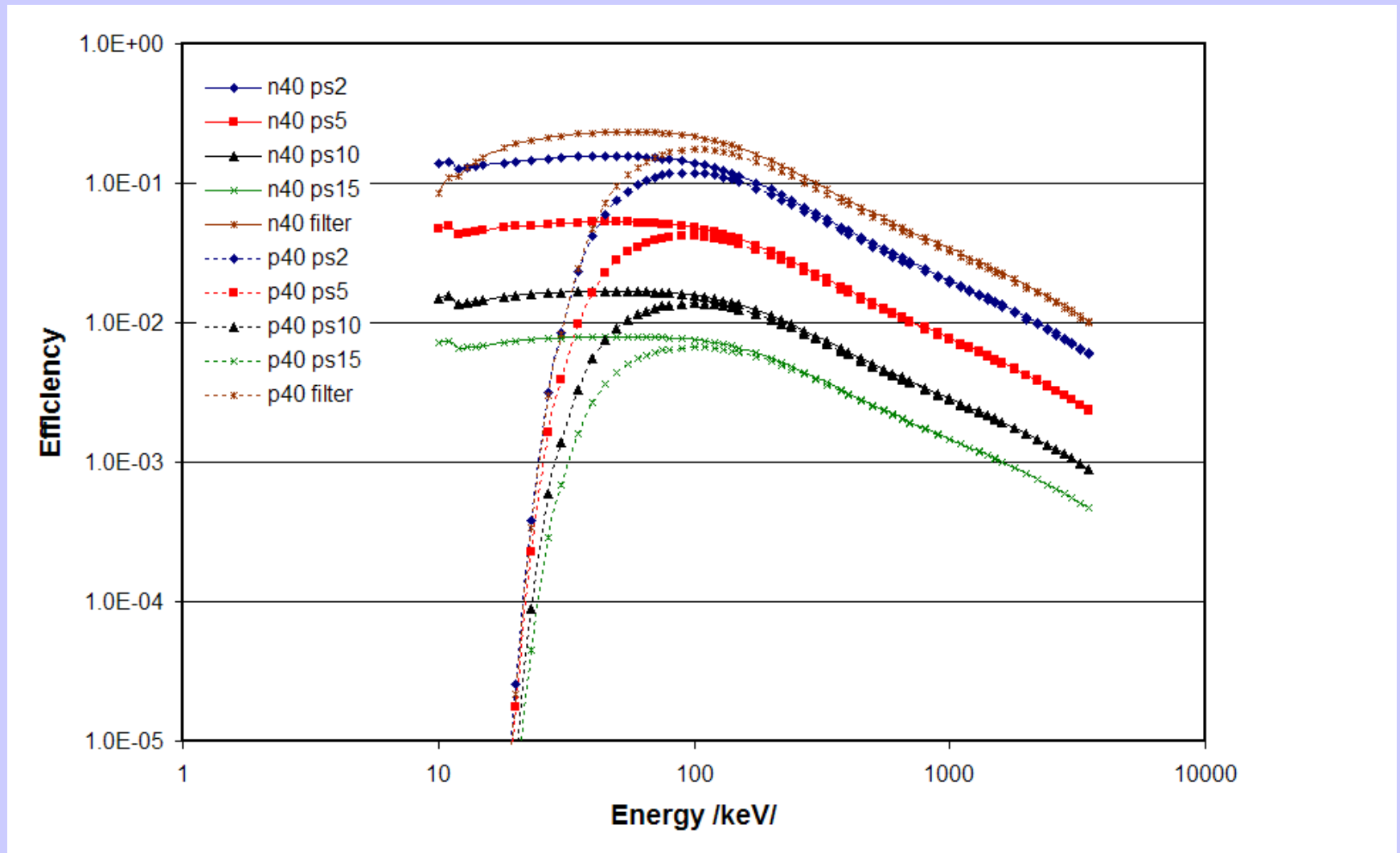
- Check if and what approximations are included
- Test validity by comparison with selected experimental results

In the case of general purpose programs, especially if user intervention required:

- Check source definition (attention at position and direction sampling!)
- Geometry, materials
- ⇒ May require programming and recompilation
- Selection of appropriate databases (energy grid), processes to be included, energy cut-off

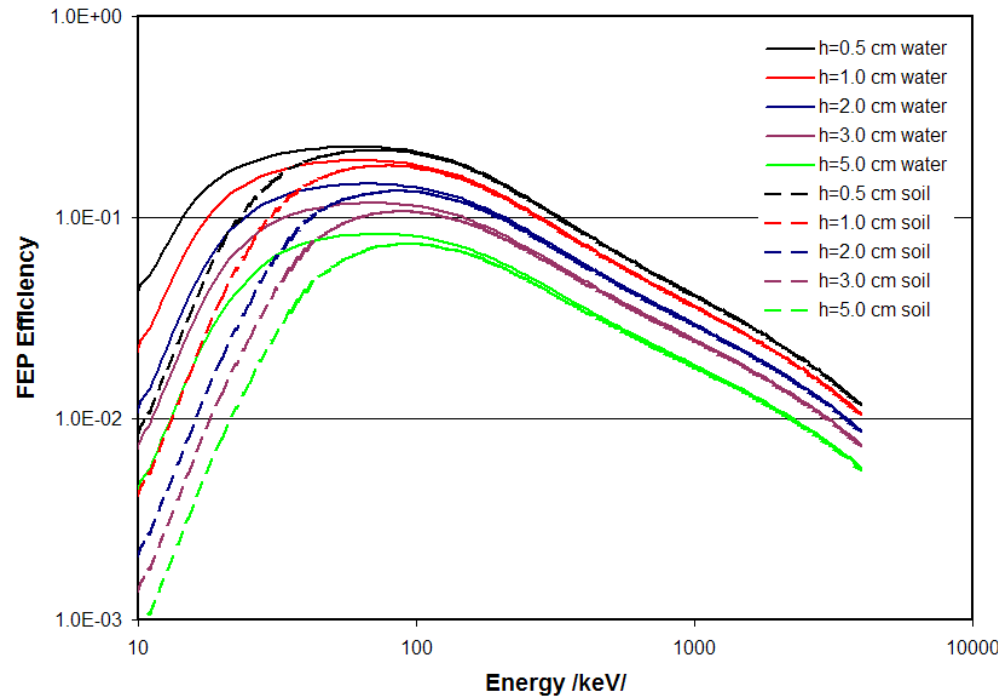
- Check the correct functionality:
 - Compare with test simulations
 - Compare with selected test measurements

Examples:



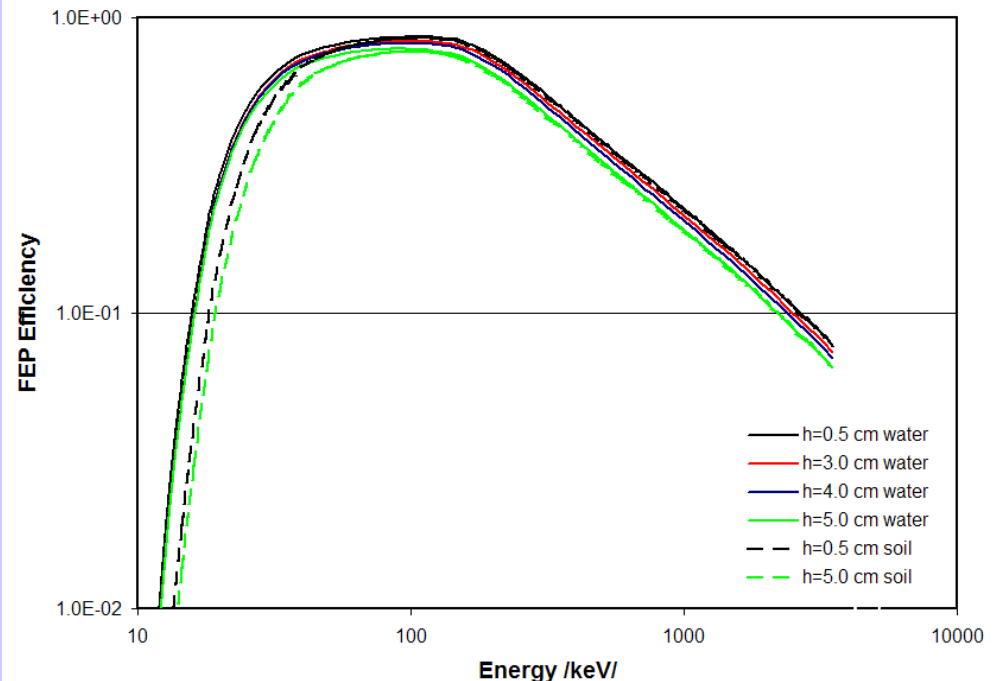
FEP efficiency computed by Monte Carlo for a p-type (p40) and an n-type (n40) HPGe detector of 40% efficiency. Sources: a filter R=2.5 cm placed on the end cap (filter) and point sources at 2 cm (ps2), 5 cm (ps5), 10 cm (ps10) and 15 cm (ps15) from the end cap, on detector axis

Efficiency curves for different values of the filling heights of water and soil samples measured with a 60 % relative efficiency n-type detector



FEP efficiency computed for water samples with $R=0.4$ cm and various filling heights h , measured with a 350 cm^3 well-type detector. The depth of the well is 5.6 cm

- Very high efficiency
- Weak sensitivity to the geometry (h) of the sample



3. Efficiency transfer from the reference to the actual measurement

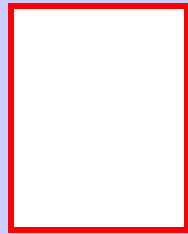
Principle:

The peak efficiency for the actual measurement configuration $\varepsilon(E, a)$ is obtained by multiplying the experimental efficiency $\varepsilon(E, ref)$ for a reference measurement configuration with the efficiency transfer factor T .

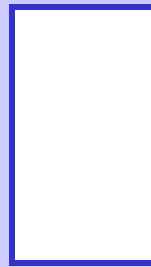
$$\varepsilon(E, a) = T(E, a, ref) \cdot \varepsilon(E, ref)$$

- T can be computed with smaller uncertainties than directly the efficiency
- T can be evaluated with different methods, robust estimation
 - Can be obtained also with methods in which the efficiency is not evaluated
- The method was proposed by L. Moens et al., NIM 187 (1981) 451 – the effective solid angle method
 - The efficiency for a volume source computed on the basis of a point source measurement
 - Transfer factor evaluated as the ratio of the corresponding effective solid angles; hypothesis: the ratio of the peak efficiency to the virtual total efficiency is independent of geometry
 - The virtual total efficiency computed much easier than the peak efficiency or the real total efficiency

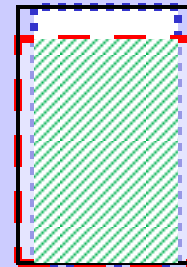
- Transfer factor in case of similar geometries:
 - Robust estimation, using a correlated sampling technique
 - Simulation of emission points in a volume containing both sources (black box)
 - Simultaneous computation of efficiency for each geometry (a , ref) if the sampled emission point is common to both (hatched volume)
 - Smaller uncertainty of T (contributions to uncertainty only of the points outside of the common volume)
 - Faster computation



Actual geometry



Reference

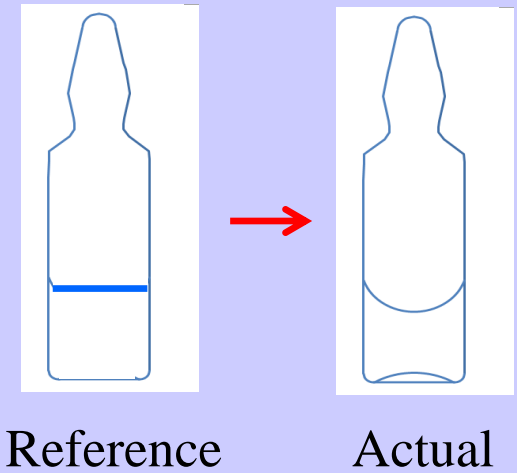
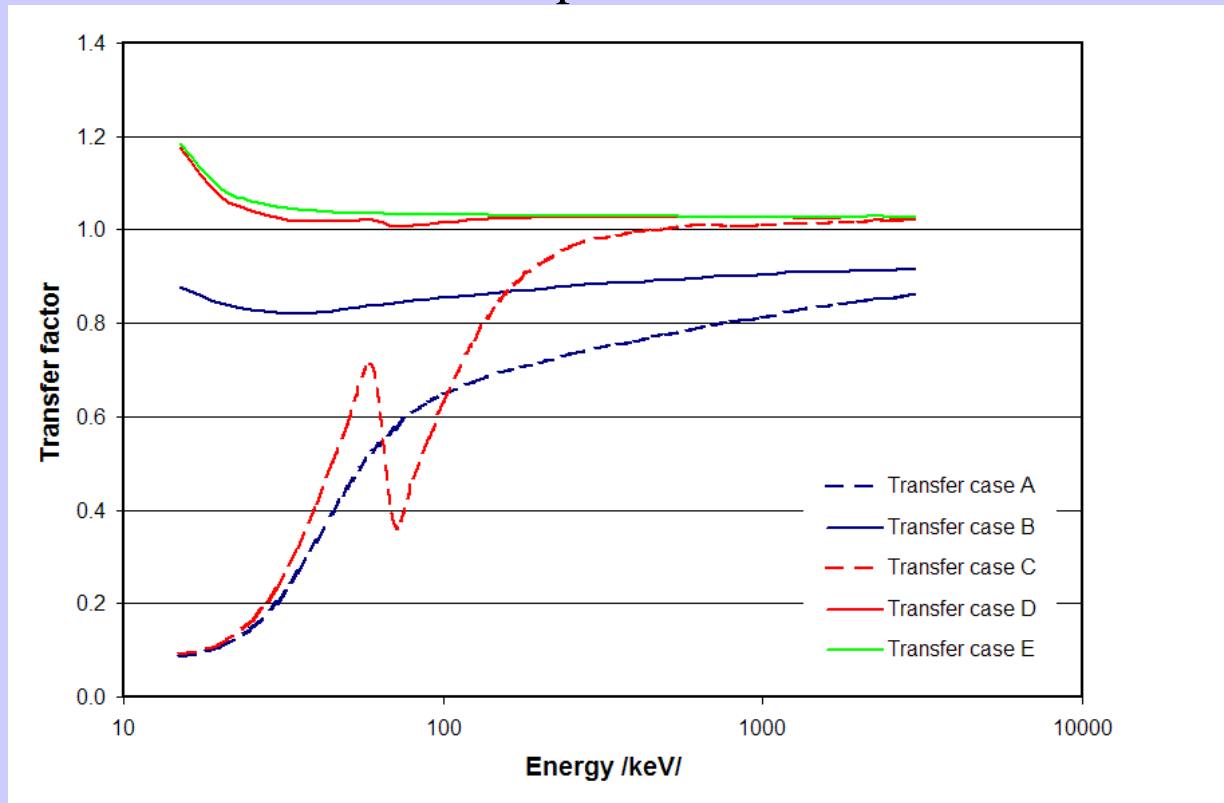


Simulation

- actual geometry slightly different from the reference geometry

Examples:

- Reference: cylinder => actual: parallelepiped
- Reference: ampoule without meniscus => actual: with meniscus



Transfer cases in Fig: Cylinder => parallelepiped: water => concrete (A); water => water (B).
 Ampoule without meniscus => ampoule with meniscus: water => $\text{Lu}(\text{NO}_3)_3$ solution (C);
 $\text{Lu}(\text{NO}_3)_3$ solution => $\text{Lu}(\text{NO}_3)_3$ solution (D); water => water (E).

4. Special Applications

- Non-uniform sources:
 - Radon distribution due to diffusion in a bulk sample
 - Radon distribution in the PTB ampoule with ^{226}Ra solution
 - ^{60}Co and ^{134}Cs point sources embedded in a bulk sample
- Compton-suppressed spectrometers
- The dead layer problem in p-type detector simulation

Non-uniform activity distribution in the source

Origin of non-uniform distribution:

- Radon diffusion – samples in improper containers
- Geological composition (in situ)
- Neutron self-shielding in neutron activation analysis
- Source preparation

Non-uniform distribution of activity => correction of the efficiency with respect to the case of a uniform source

If activity distribution is known, efficiency correction can be computed by simulation

Effect of intrinsic inhomogeneity – see Special Problems in Self-Attenuation – ARI 126 (2017) 146; ARI 134 (2018) 137

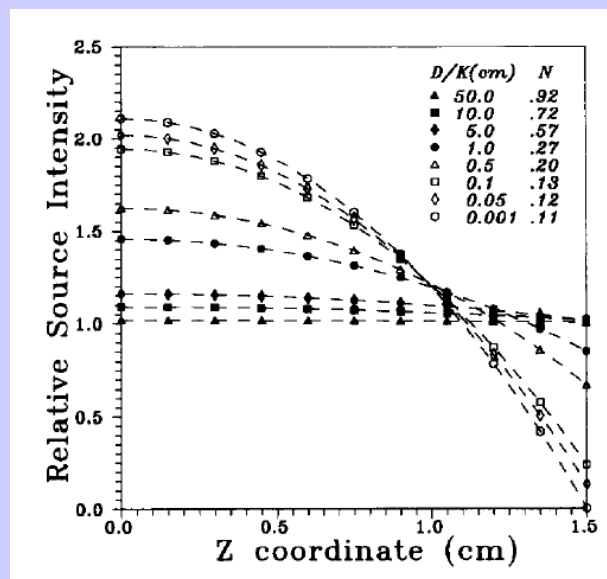
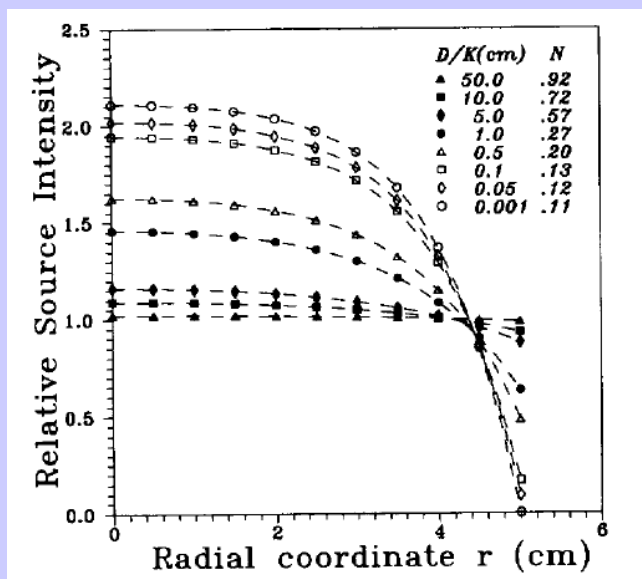
Radon distribution in a bulk soil sample – diffusable fraction – depends on:

- Diffusion coefficient D
- Permeability of the walls – boundary value K

The diffusion equation can be solved analytically

Consequences of diffusion and leakage:

- Lower activity of radon in the sample due to leakage (radon no longer in equilibrium with parent nuclide)
- Spatial activity distribution no longer uniform – higher distortion in the case of ^{220}Rn than ^{222}Rn due to shorter decay time)



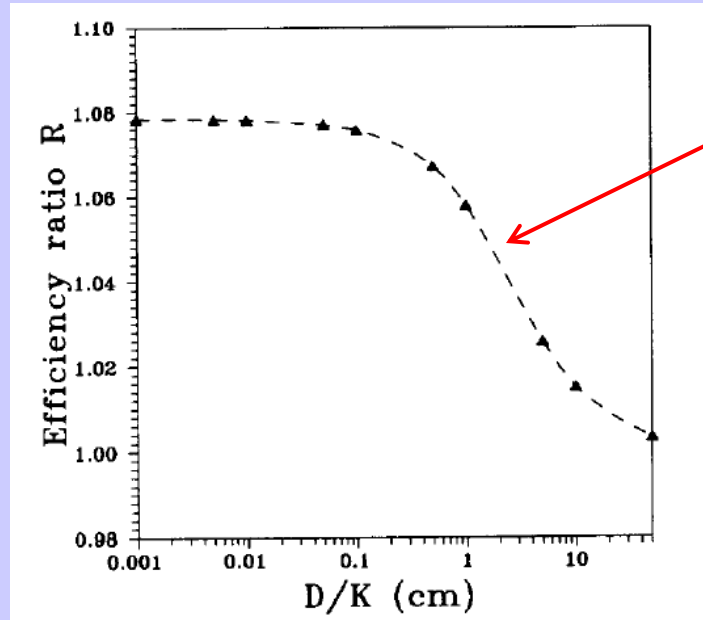
Source:
Sima, ARI 47 (1996) 919

^{220}Rn distribution due to diffusion through sample and leakage

Soil sample in cylinder with R=5 cm, H=3 cm. D=0.05, various values of K

Effect of ^{220}Rn leakage:

- Decreased activity in the sample
- Modified efficiency for the activity remaining in the sample



Efficiency correction factor for the 239 keV peak of ^{212}Pb

- The effect of leakage on spatial distribution of ^{222}Rn less pronounced
- However, if the container is not completely filled (air above soil) => radon diffusion in air very important - Carconi et al, ARI 70 (2012) 2119 – correction factor 20% if container filled about 70%.

More complex case – ^{226}Ra solution in an incompletely filled ampoule – see below

Neutron self-shielding in high volume samples irradiated in view of neutron activation analysis => non uniform activation => effect on efficiency

- Efficiency correction up to 5% for a polyacetal sample with $R=5$ cm, $H=10$ cm, $\rho=1.54$ g cm^{-3} (Sima, JRNC 244 (2000) 669)

^{226}Ra solution in the PTB ampoule

Ott et al., ARI 87 (2014) 365

^{226}Ra solution incompletely filling the ampoule represents a complex source, with complex distribution of activity

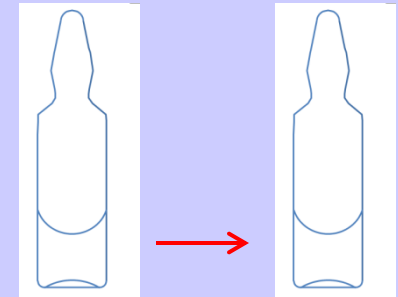
^{222}Rn is partly in solution, partly in the gas

^{222}Rn decay products in the gas may be deposited on the surfaces

How is the activity distributed?

How is the efficiency in various geometries affected?

- in particular, what corrections should be applied in order to use efficiency calibration with the ampoule coaxial with the detector, in the standard distance (18.5 cm) for the activity assessment of other ampoule sources, with uniform activity distributed only in solution?



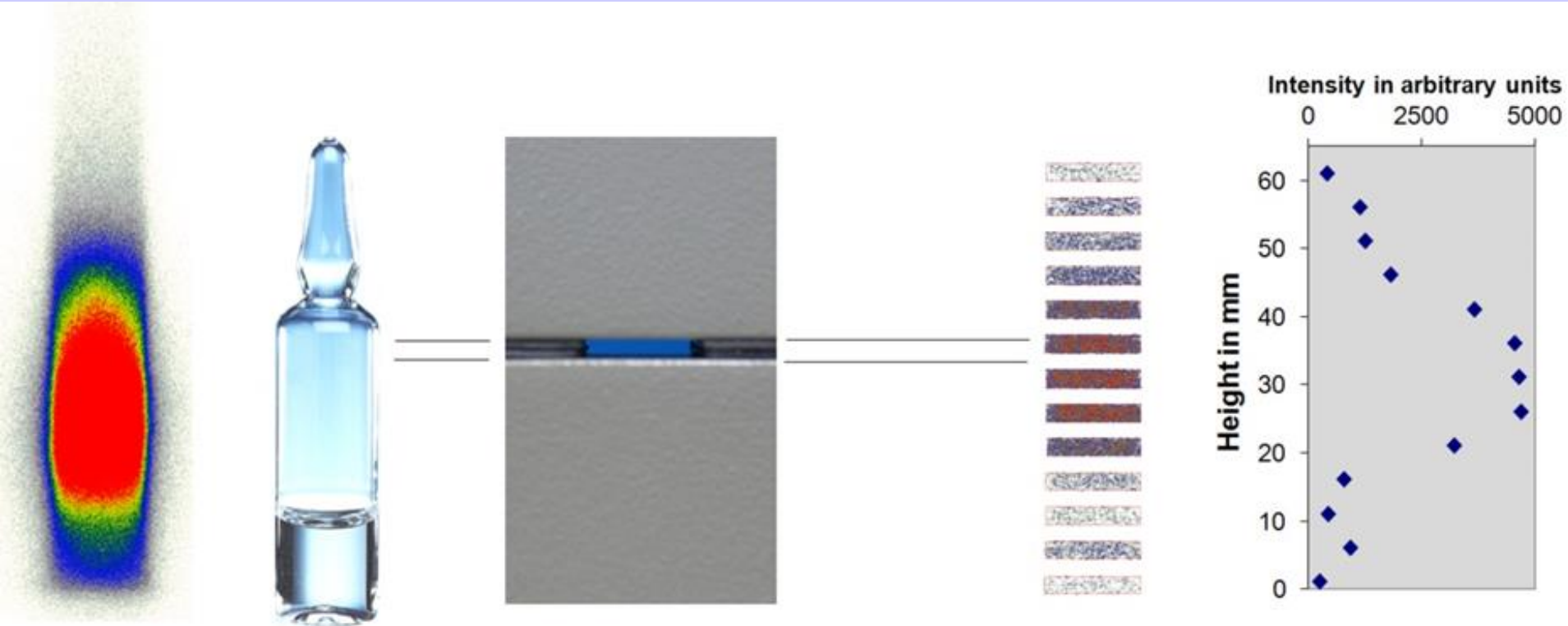
^{226}Ra
standard

other
source



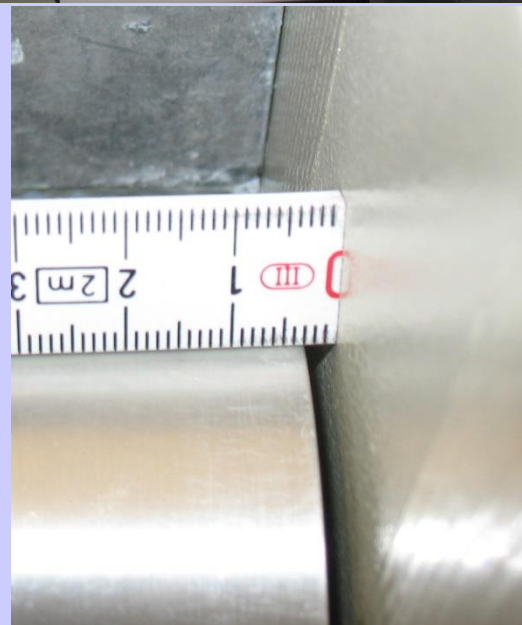
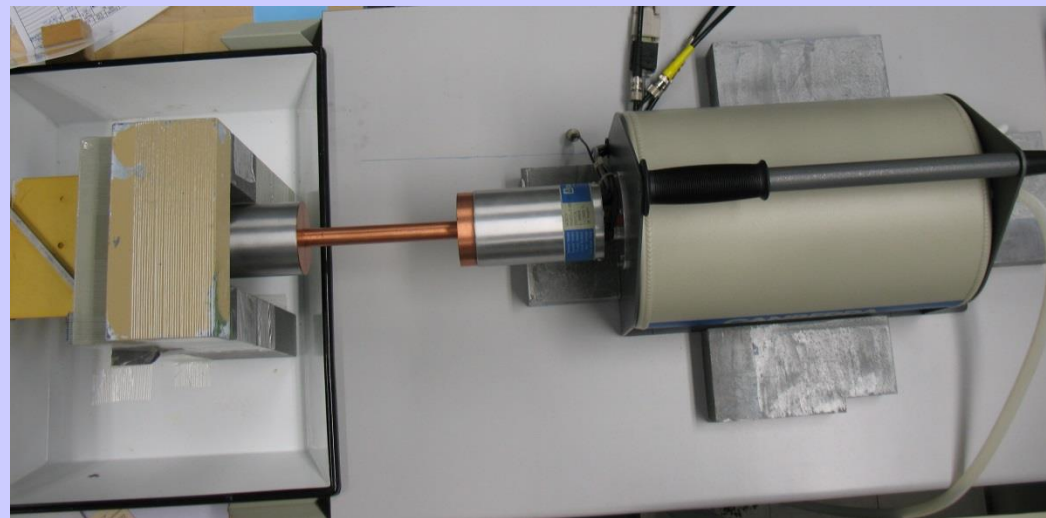
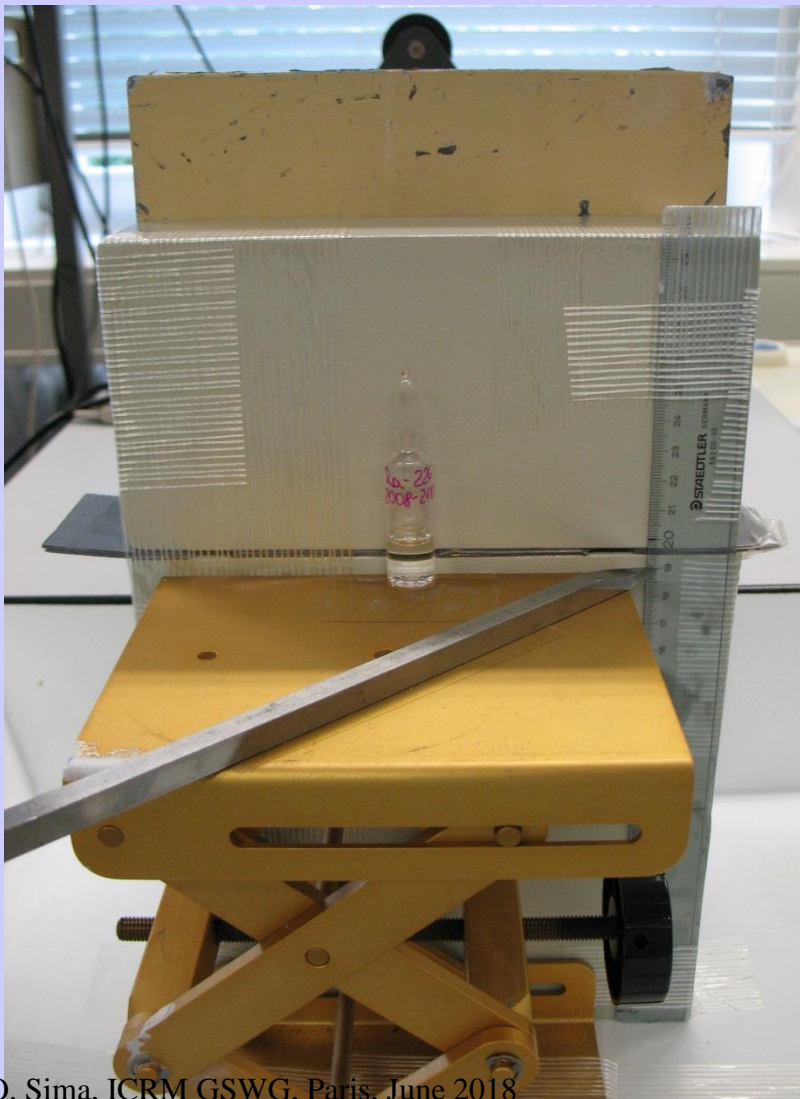
Efficiency
transfer

First measurements:
Autoradiography of the ampoule
Autoradiography in specific sections, with a slit diaphragm

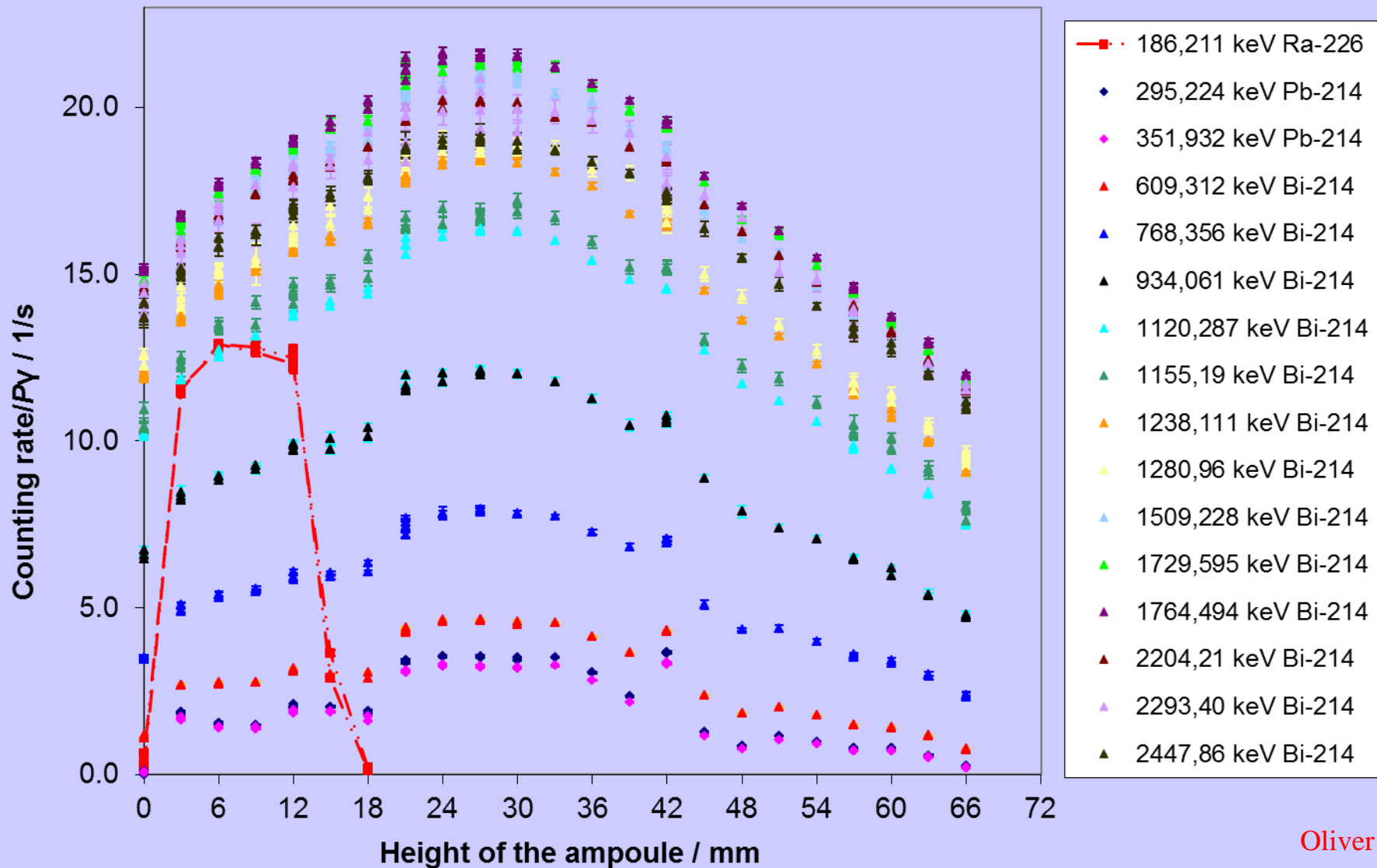


Oliver Ott

Experimental set-up of the HPGe detector system including slit diaphragm.
Standard measurements: slit of 2.4(1) mm x 16.1(1) mm; smaller slit: 2.4(1) x 6.4. Pb shielding: 50 mm



Oliver Ott



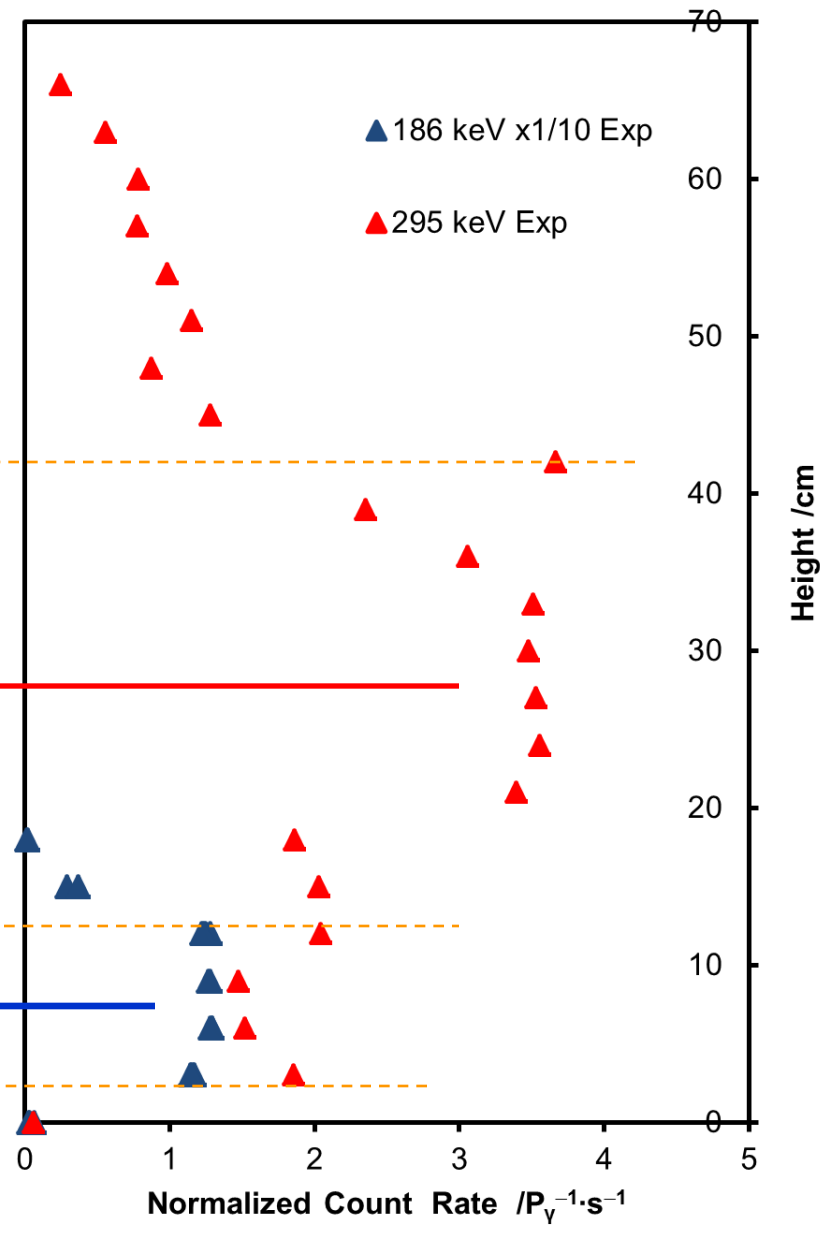
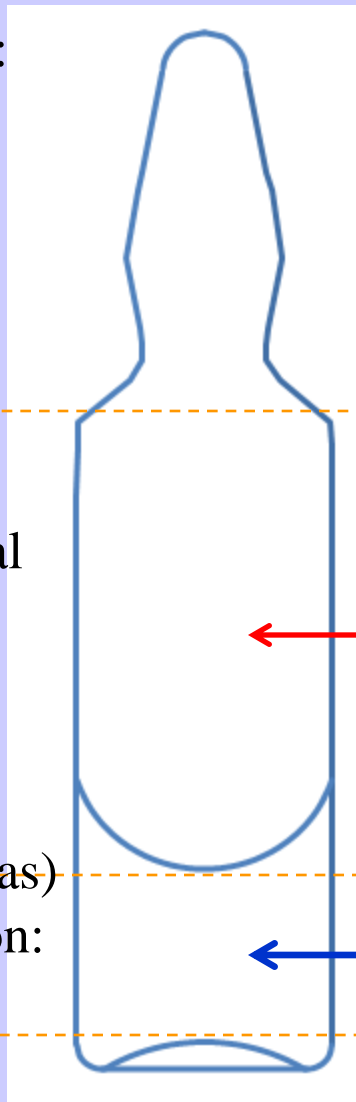
Oliver Ott

Normalized count rates in the peak of ^{226}Ra (line) and of radon decay products

Most relevant information:
count rate in 295 keV vs
186 keV

Decay products in gas
compartment

- Count rate proportional to area seen through the slit
- Ratio for slit width 6.4 and 16.1: 0.183 (solution) and 0.114(gas)
- MC uniform in solution: 0.193; on solution surface: 0.108
- MC uniform on gas surface: 0.095; uniform in volume: 0.165



Simulations with GESPECOR:

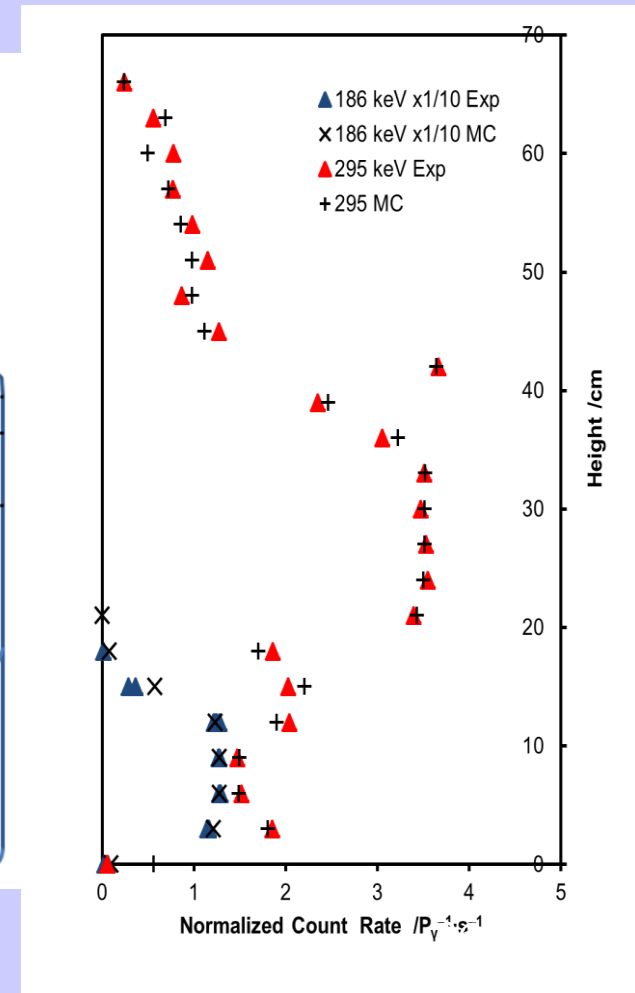
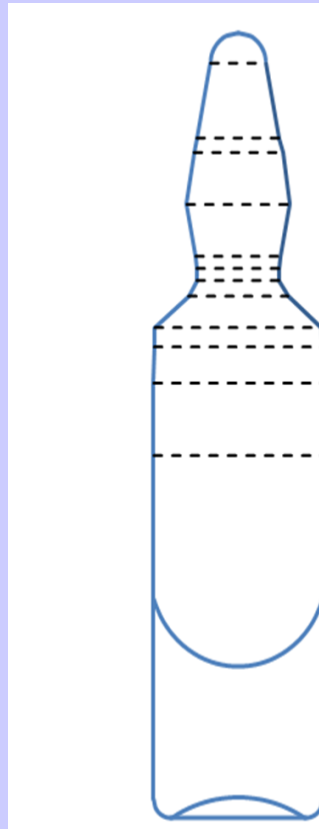
- Geometrical model of the ampoule, extension of basic shapes and volumes (truncated cones, segments of sphere)
- Simulation of uniform emission from the volumes
- Simulation of uniform emission from the surfaces

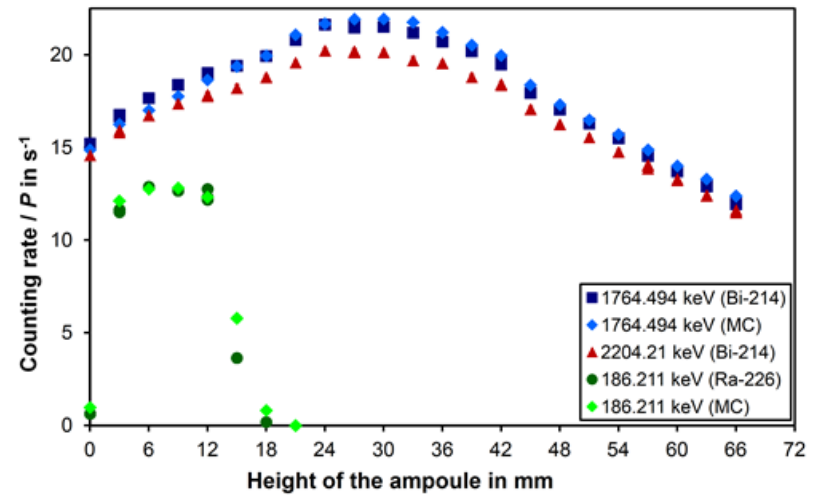
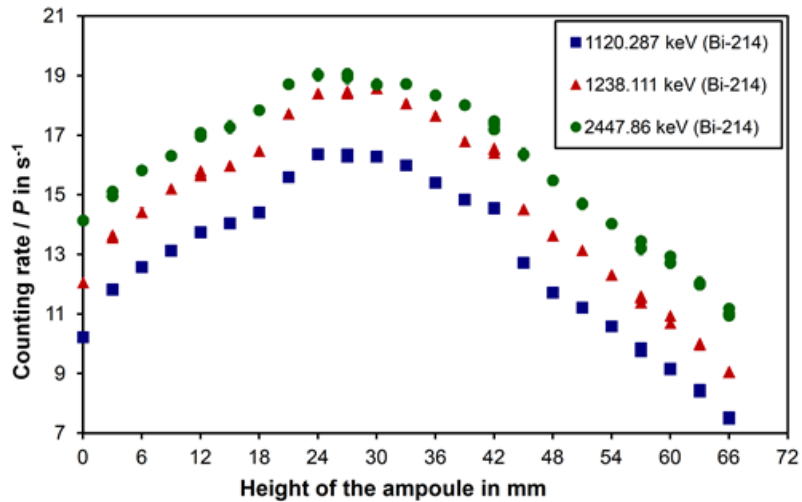
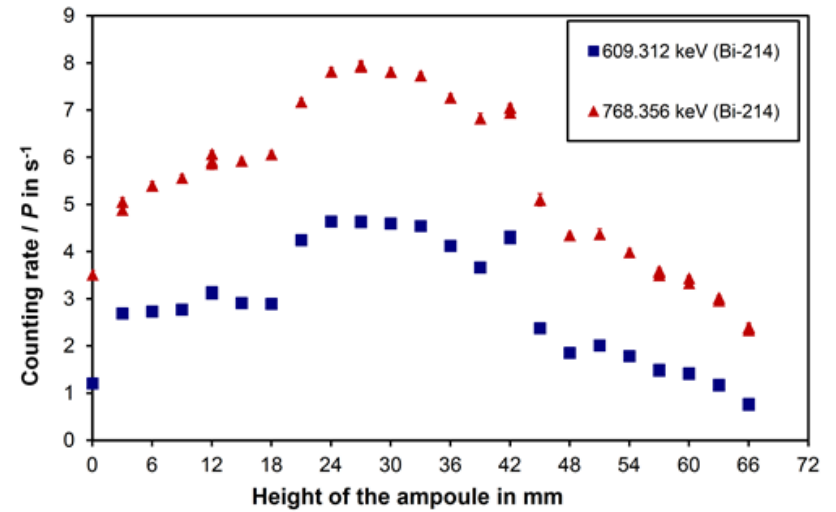
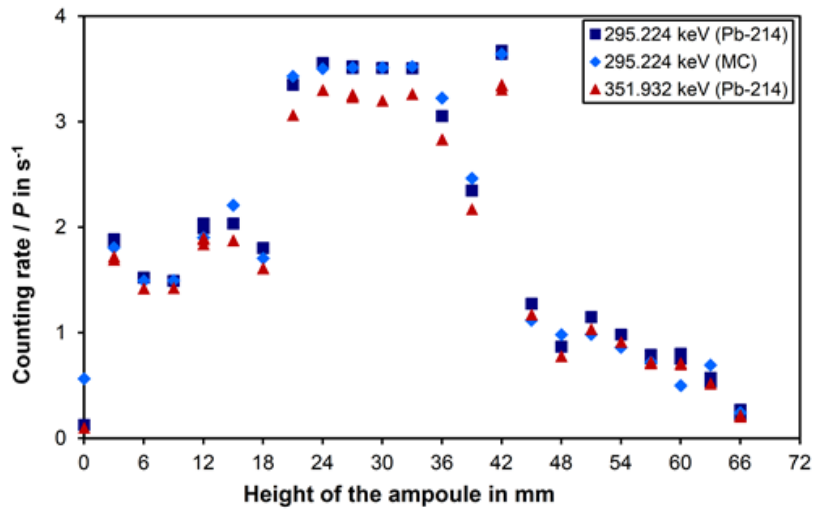
Already existing extensions:

- Rounded edges of the ampoule
- Central bump in the bottom
- Meniscus

Source distribution required

- Agreement between simulation and experiment for 295 keV of ^{214}Pb obtained if:
- Basically ^{214}Pb is uniformly distributed in the solution and uniformly distributed on the surface of the gas compartment
- Distortions close to surface changes
- Partial deposition on meniscus
- After adjustment of distribution of ^{214}Pb , all data well reproduced by simulation





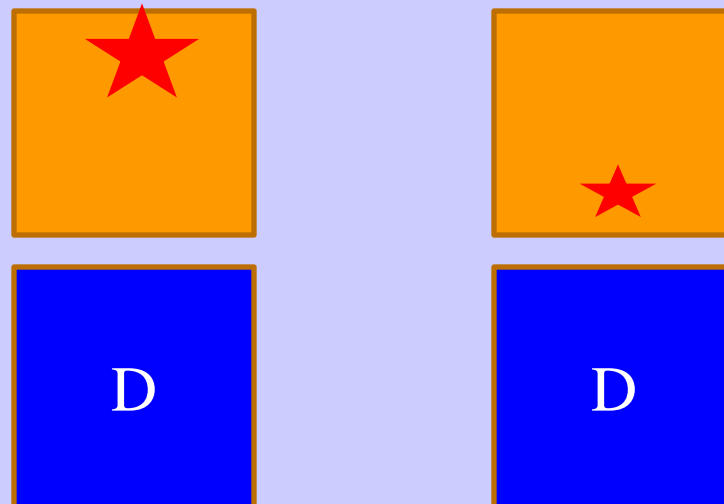
^{60}Co and ^{134}Cs point sources with unknown position in a bulk sample
(Suvaila et al., ARI 81 (2013) 76; Suvaila et al., ARI 87 (2014) 384)

If a point source is located in an unknown position in a bulk sample (e.g. a hot particle) the computed activity may be biased

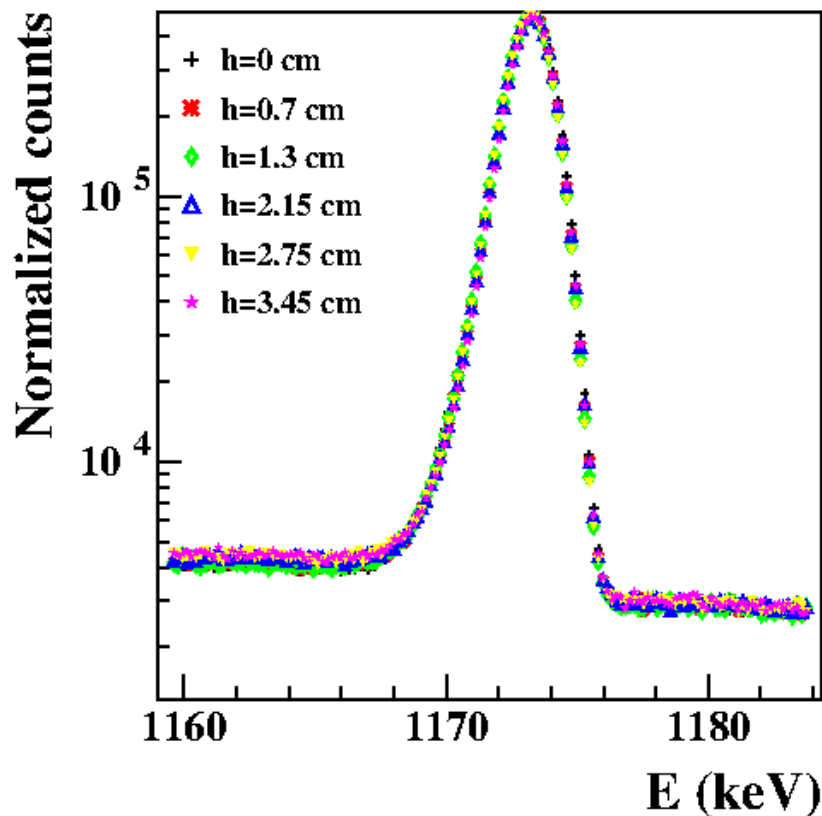
How to get information on source position from the spectrum?

- For nuclides with important sum peaks the ratio of the count rate from the sum peak and from a normal peak is sensitive to source position

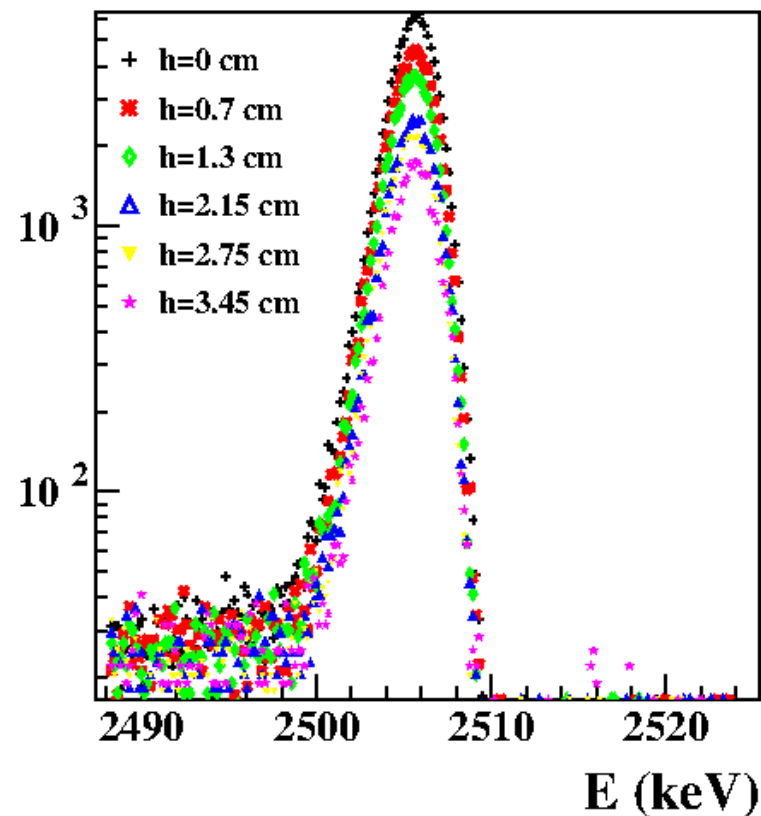
In the figure, the same count rate in the main peaks can be obtained for a higher activity source located farther from the detector as for a lower activity source located closer to detector



1173 keV



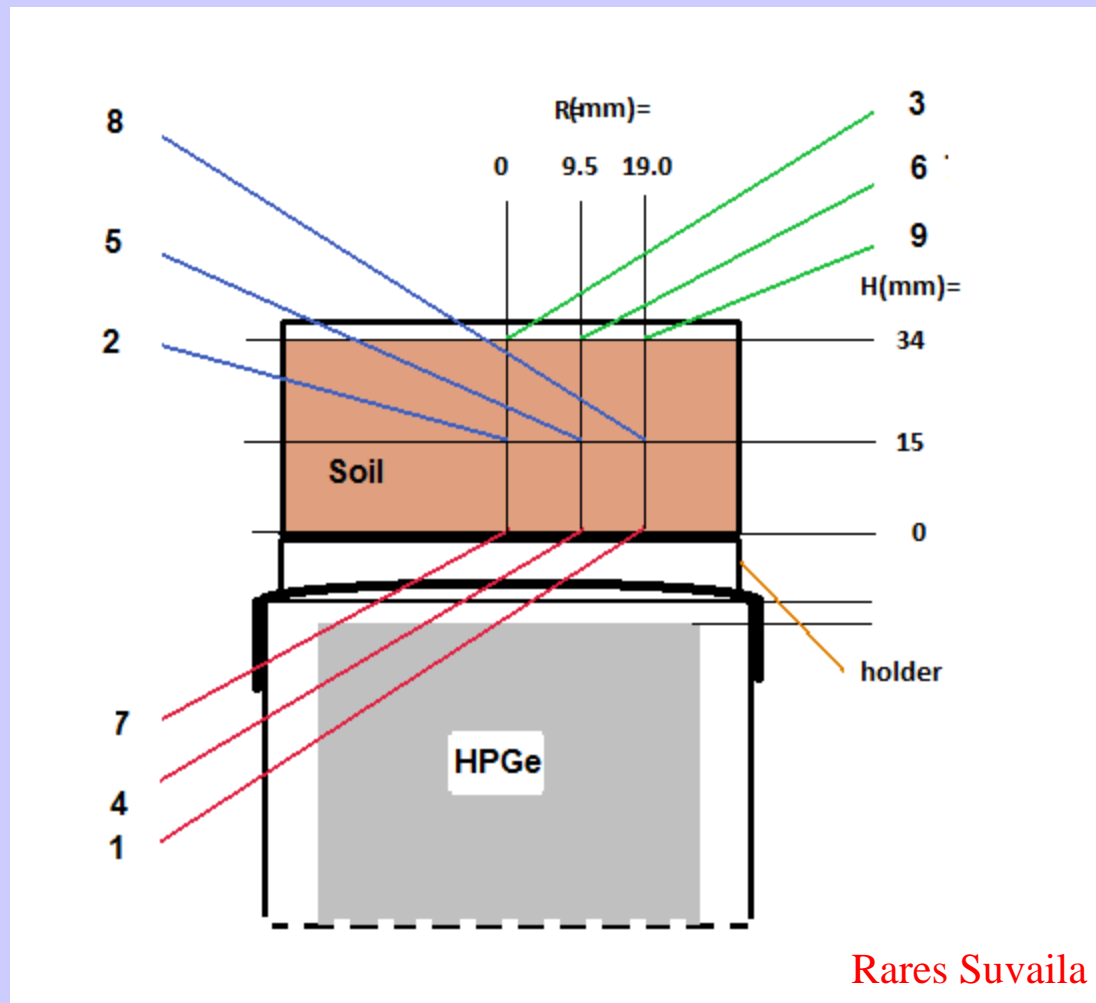
2505 keV Sum Peak



Counts in the peaks of 1173 keV and sum peak (2505 keV) normalized to the counts in the 1332 keV peak, for various distances h of the point source from the detector

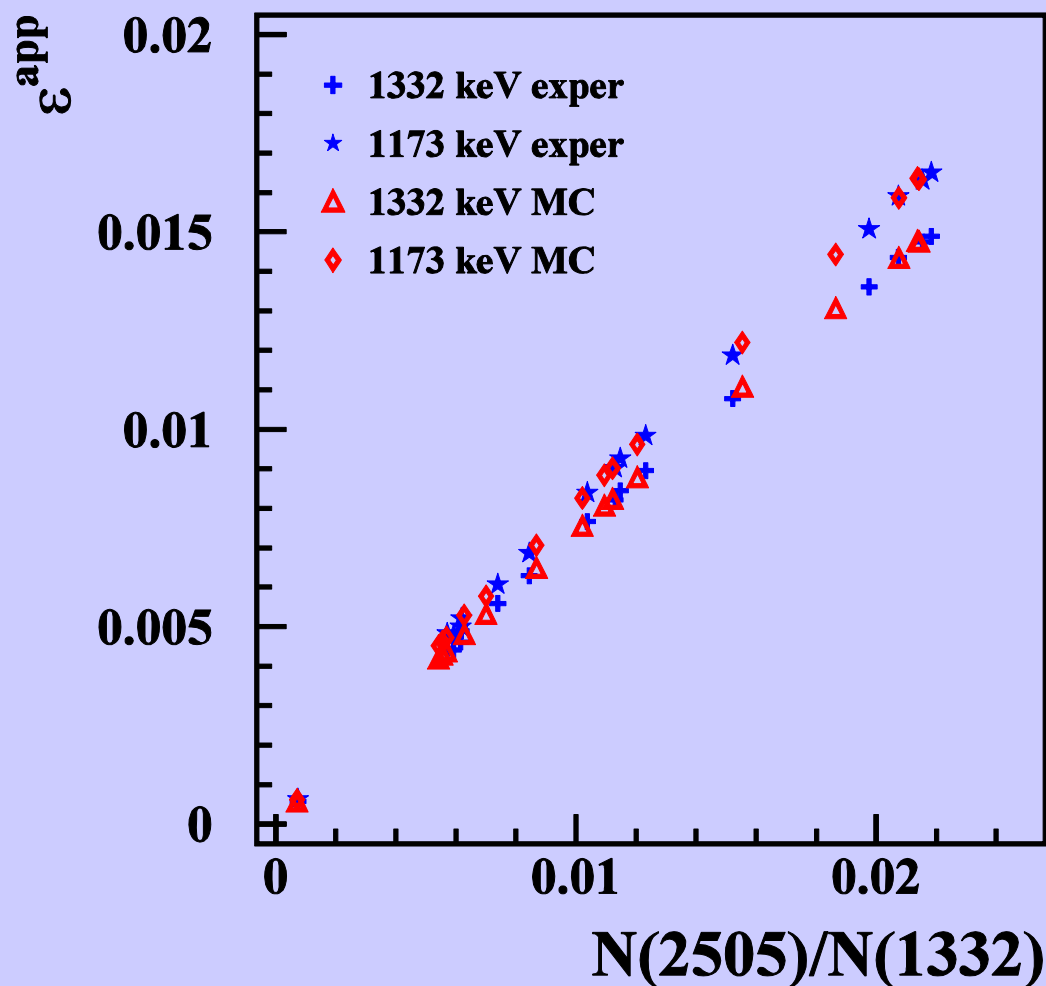
\Rightarrow Ratio $R(2505)/R(1332)$ much more sensitive to source position than ratio $R(1173)/R(1332)$

Measurements: ^{60}Co point source placed in several positions in a soil sample



Ratio of the count rate in the sum peak to the count rate in the peak of 1332 keV strongly correlated with the apparent efficiency at 1173 keV

=> Correlation pattern very robust



R (mm)	h (mm)	1173 keV	1332 keV	2505 keV	Sum Peak	Correlation
0	1	5100	5101	4935	5272	5273
0	7	5102	5102	4998	5208	5300
0	13	5356	5348	5471	5236	5367
0	21.5	5092	5085	4950	5232	5332
0	27.5	5512	5507	5818	5217	5323
0	34.0	5472	5461	5632	5306	5337
0	1	5284	5284	5397	5174	5201
9.5	1	5384	5391	5599	5184	5209
19	1	5471	5458	5781	5165	5235
0	15	5383	5377	5506	5257	5403
9.5	15	5345	5339	5512	5177	5333
19	15	5326	5321	5410	5239	5383
0	34	5502	5489	5759	5243	5291
9.5	34	5539	5531	6002	5105	5176
19	34	5528	5533	6058	5048	5110
	Mean	5360	5355	5522	5204	5285
	Std. Dev.	151	149	339	63	81
	% Std. Dev.	2.8	2.8	6.1	1.2	1.5

Activity computed using parameters obtained through different methods:

Columns 2-4: peak efficiency computed for the specific position of the source

Column 5: correction factors computed for the specific position of the source

Column 6: peak efficiency computed from correlation pattern and measured $R(2505)/R(1332)$

Source: ARI
81 (2013) 76

Extension to samples with inhomogeneous matrix – Suvaila et al., ARI 87 (2014) 384

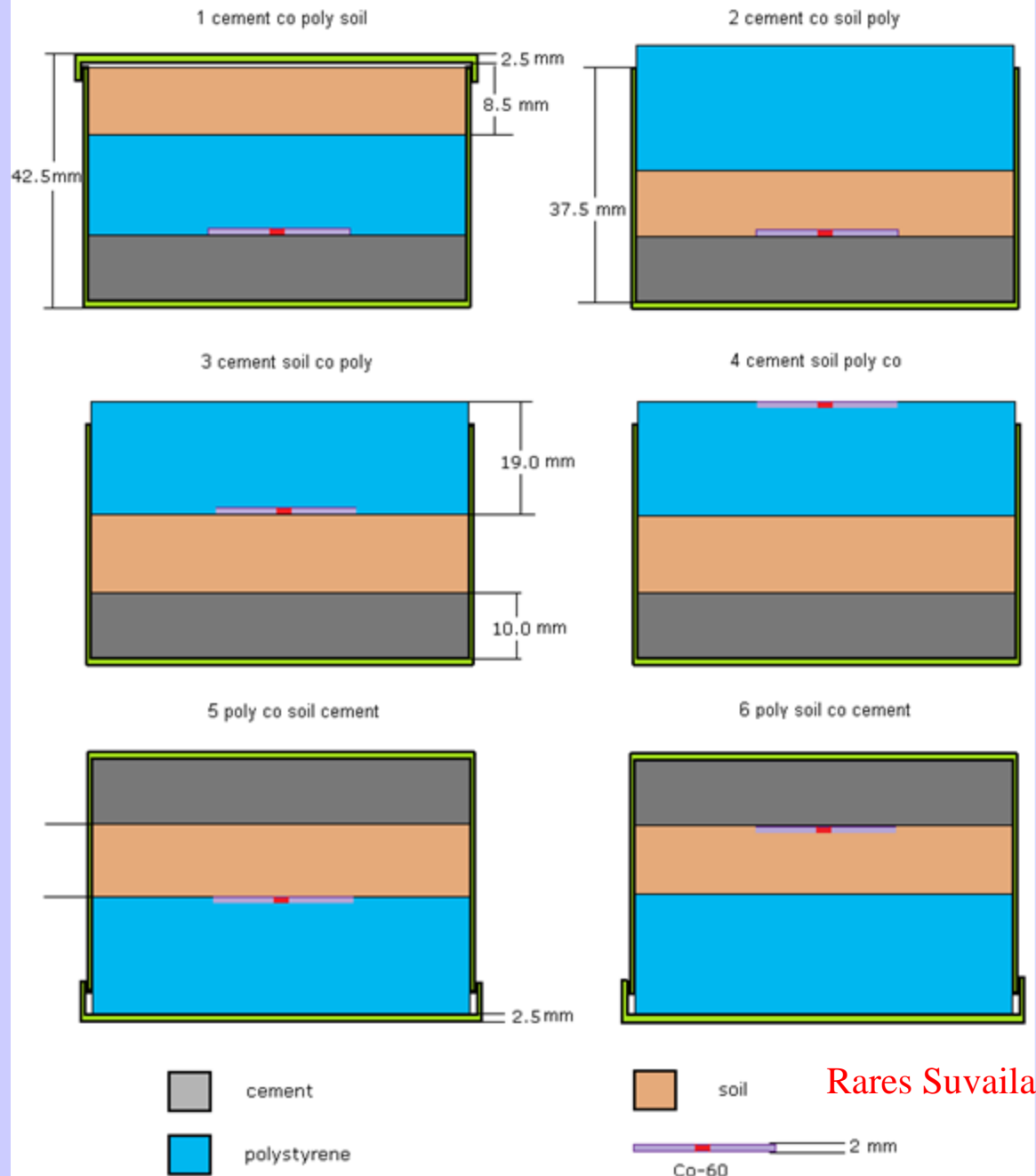
- 3 layers in various orders:

Soil $\rho=1.3 \text{ g cm}^{-3}$

Cement powder $\rho=1.55 \text{ g cm}^{-3}$

Polystyrene $\rho=0.32 \text{ g cm}^{-3}$

Source placed between layers



Sample no.	1173 keV ^(a)	1332 keV ^(a)	Sum Peak ^(b)	1173 keV ^(c)	1332 keV ^(c)	Sum Peak ^(d)	Correlation ^(e)
1	5276	5273	5126	8209	8176	4655	5188
2	5500	5498	5107	8525	8487	4593	5137
3	5493	5487	5196	4834	4861	5072	5341
4	5221	5217	5178	2958	2983	5263	5114
5	5014	5010	5243	7054	6984	4904	5381
6	5030	5026	5181	4271	4260	5109	5291
Mean	5256	5252	5171	5975	5958	4933	5188
Std. Dev.	213	213	50	2280	2250	265	111
% Std. Dev.	4.1	4.1	1.0	38	38	5.4	2.2

^(a) Efficiency computed by Monte Carlo for the specific case Source: ARI 87 (2014) 384

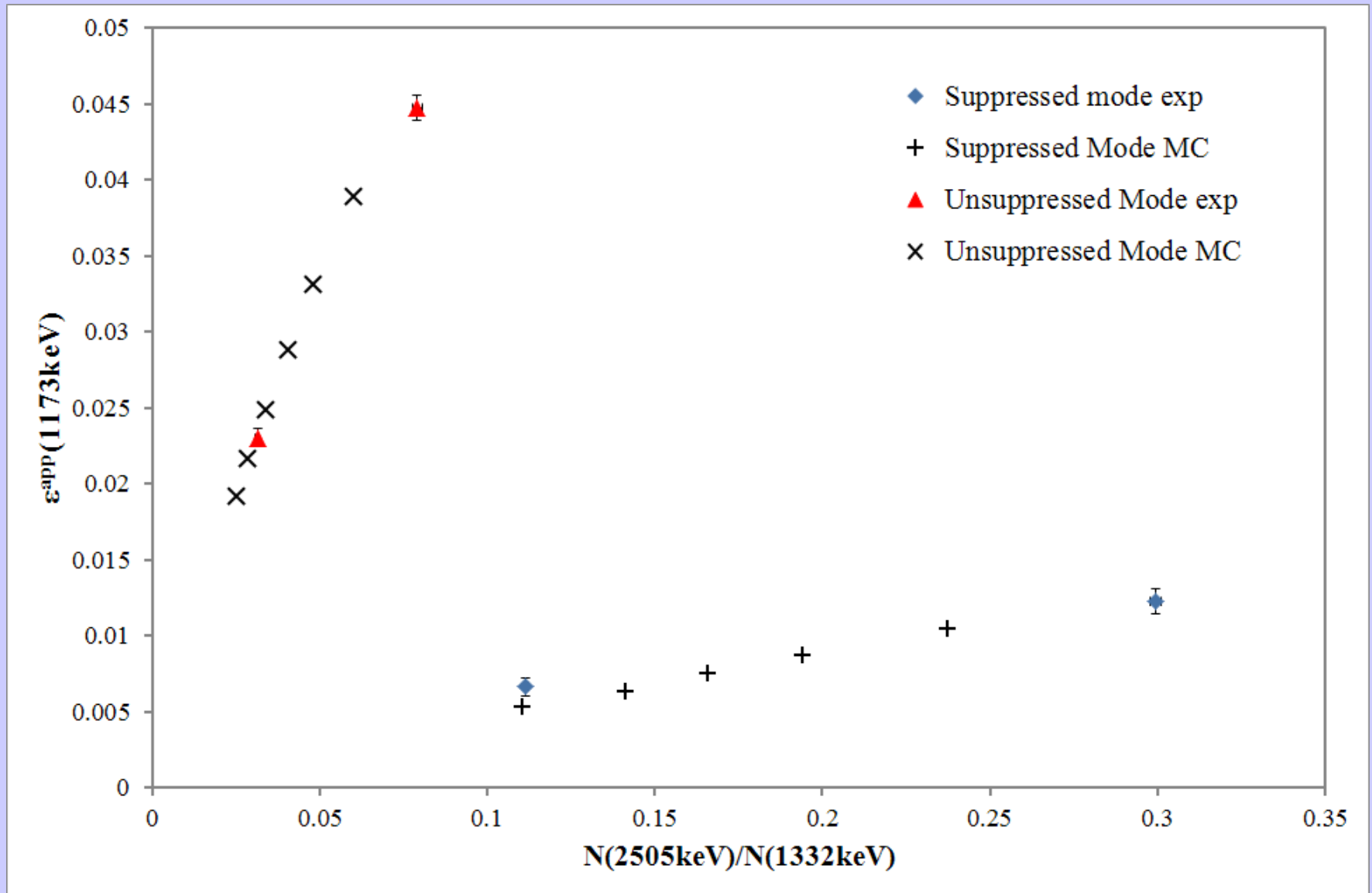
^(b) Sum peak, correction by Monte Carlo for the specific case

^(c) Efficiency by Monte Carlo, uniform activity and matrix

^(d) Sum peak, uniform activity and matrix assumed for correction

^(e) Correlation method

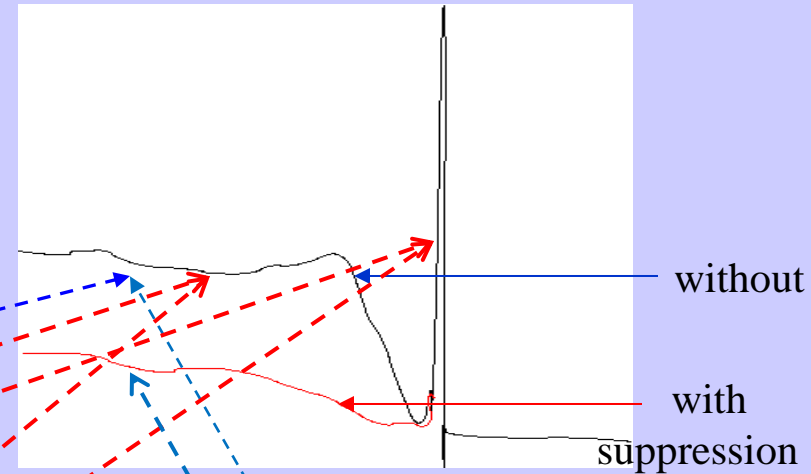
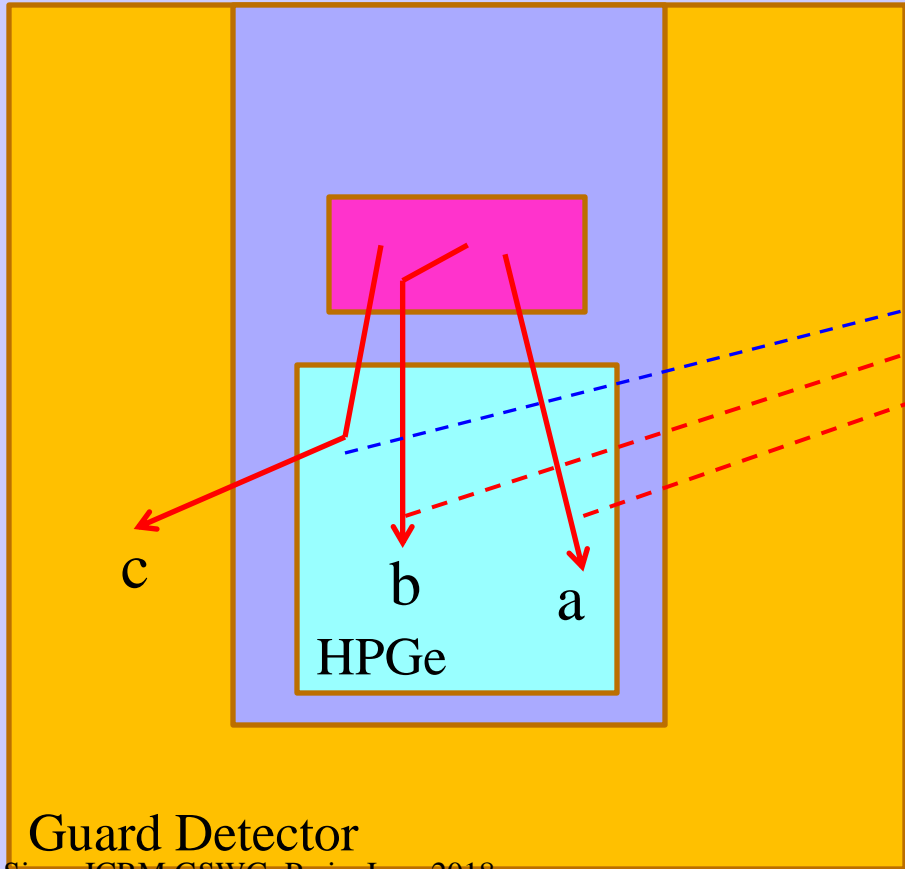
Correlation also valid in the case of Compton Suppressed spectrometers



Source: ARI 87 (2014) 384
35

Compton-suppressed spectrometers

a. Single gamma emitting nuclide

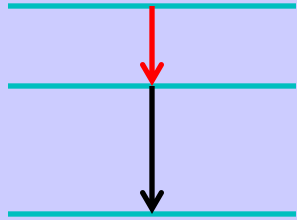


b and a events:
spectrum not affected with or without Compton suppression

c events:
without suppression => count in the spectrum
with suppression => no contribution – suppressed background

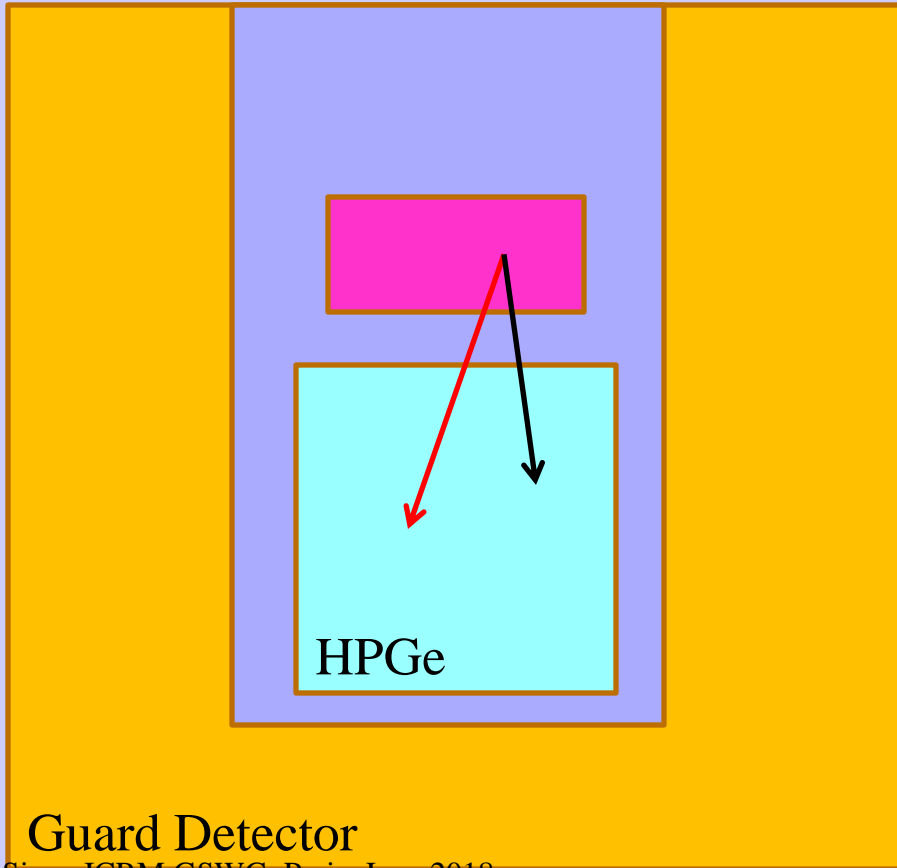
Peak count rate = not affected

b. Multigamma nuclide:



First photon; only the cases when it is totally absorbed in HPGe

Second photon, various cases



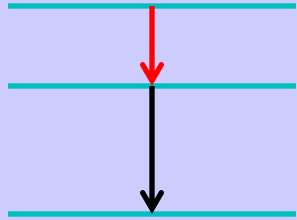
Case a

Usual coincidence losses from the peak of the first photon

No veto from Guard detector

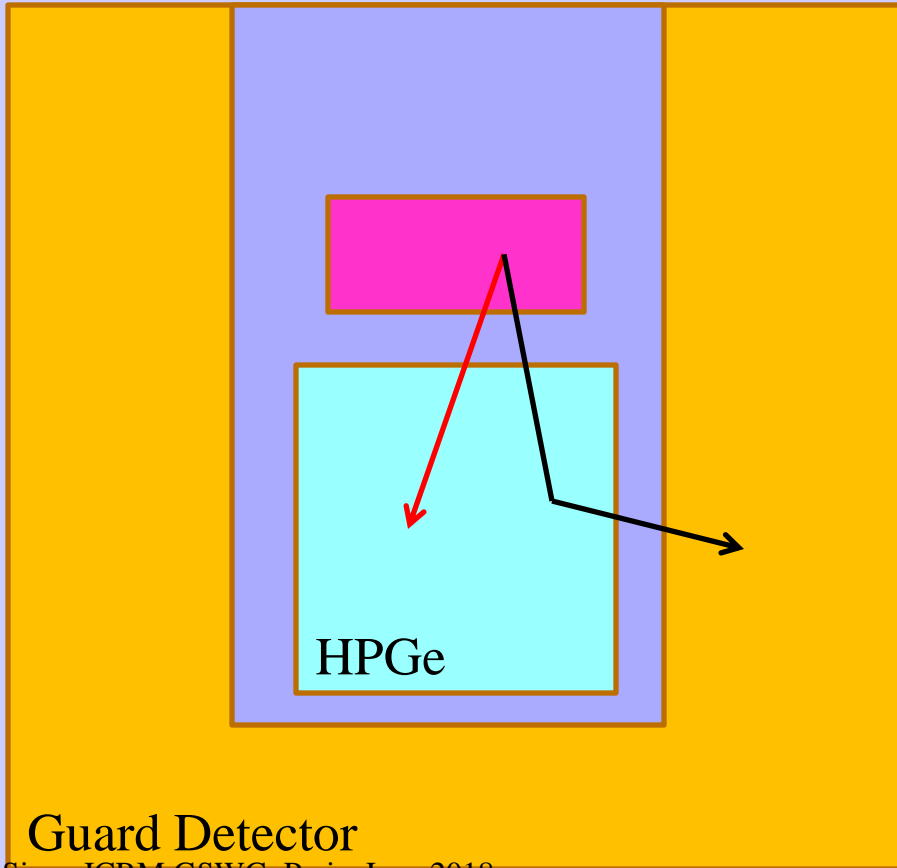
Contribution to the total efficiency of the HPGe detector, $\varepsilon_T^D(E_2)$

b. Multigamma nuclide:



First photon; only the cases when it is totally absorbed in HPGe

Second photon, various cases



Case b

Usual coincidence losses from the peak of the first photon

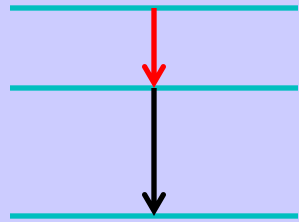
Veto from Guard detector

Contribution to the total efficiency of the HPGe detector, $\varepsilon_T^D(E_2)$

Contribution to the total efficiency of the Guard detector, $\varepsilon_T^G(E_2)$

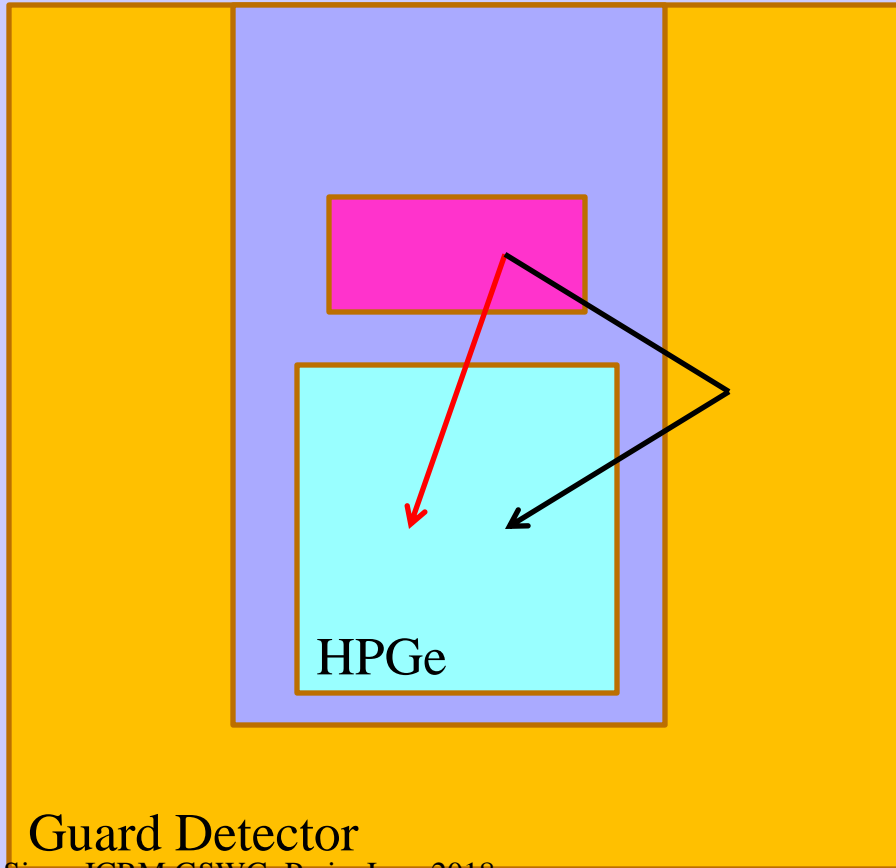
Contribution to the coincidence efficiency of detectors, $\varepsilon_T^{D+G}(E_2)$

b. Multigamma nuclide:



First photon; only the cases when it is totally absorbed in HPGe

Second photon, various cases



Case c

Usual coincidence losses from the peak of the first photon

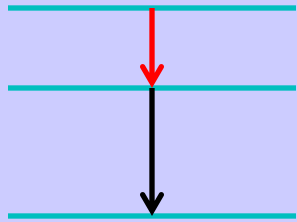
Veto from Guard detector

Contribution to the total efficiency of the HPGe detector, $\varepsilon_T^D(E_2)$

Contribution to the total efficiency of the Guard detector, $\varepsilon_T^G(E_2)$

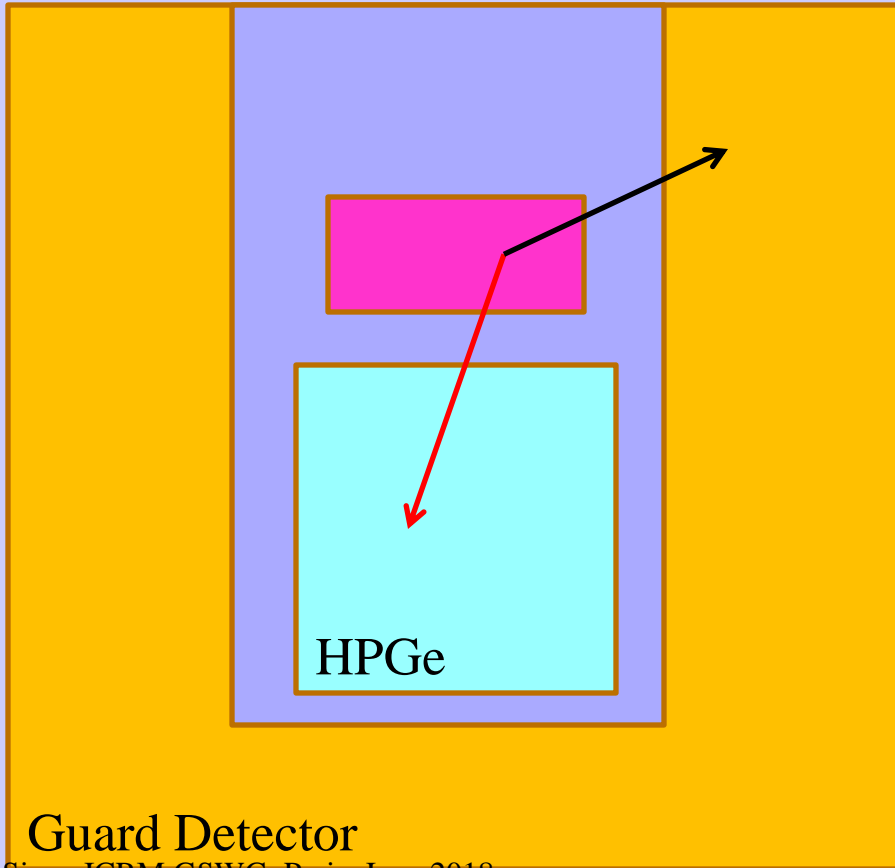
Contribution to the coincidence efficiency of detectors, $\varepsilon_T^{D+G}(E_2)$

b. Multigamma nuclide:



First photon; only the cases when it is totally absorbed in HPGe

Second photon, various cases



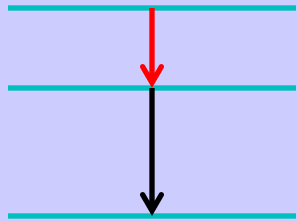
Case d

No coincidence losses from the peak of the first photon

Veto from Guard detector

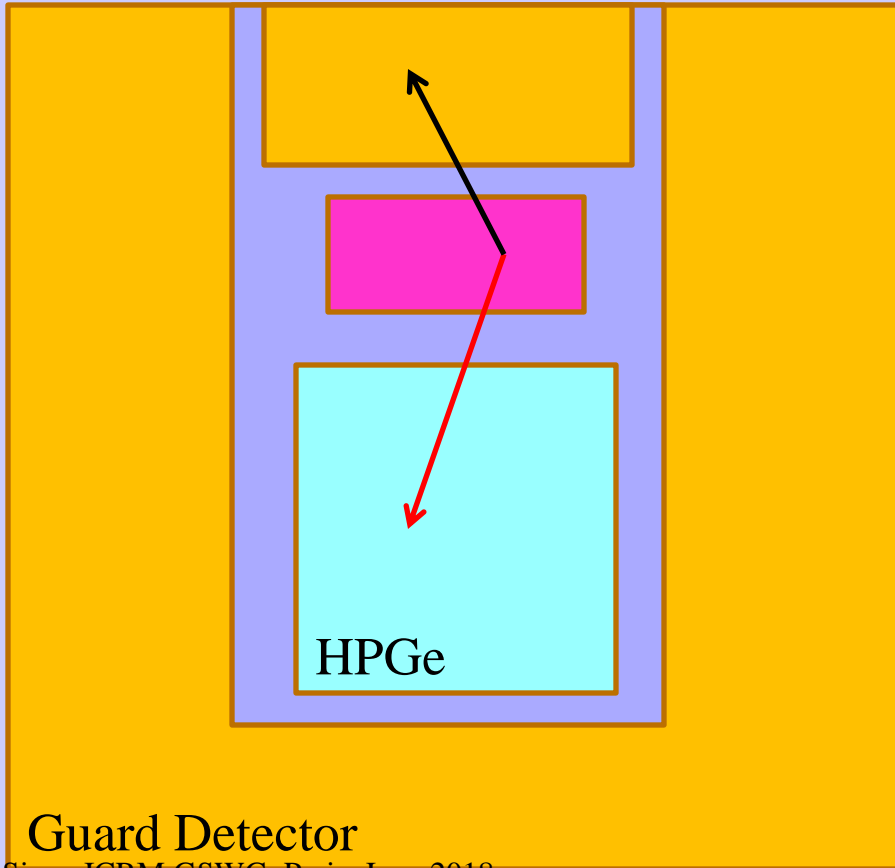
Contribution to the total efficiency of the Guard detector, $\varepsilon_T^G(E_2)$

b. Multigamma nuclide:



First photon; only the cases when it is totally absorbed in HPGe

Second photon, various cases



Case d

No coincidence losses from the peak of the first photon

Veto from Guard detector

Contribution to the total efficiency of the Guard detector, $\varepsilon_T^G(E_2)$

Multigamma nuclide:

⇒ Reduction of the background under the E_1 peak due to reduction of Compton plateau of higher energy photons (if they exist) and of the background

⇒ Coincidence losses due to the detection of other photons in the HPGe (usual coincidence losses)

⇒ Losses from the E_1 peak due to the veto of the anti-Compton resulting from all the other photons emitted together with the photon of interest

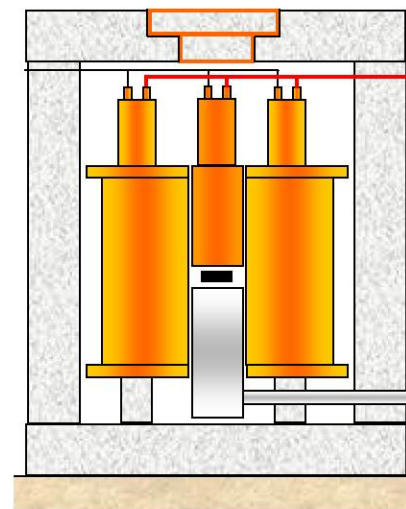
⇒ Significant decrease of the peak efficiency; correction factors depend on the nuclide decay scheme and on the particular transition

Experiment

- Measurements done in the underground laboratory of IAEA's Environment Laboratories, Monaco
- For each measurement two spectra:
 - Suppressed (Anti-Compton, AC)
 - Unsuppressed (Direct, D)

Efficiency calibration (in both modes):

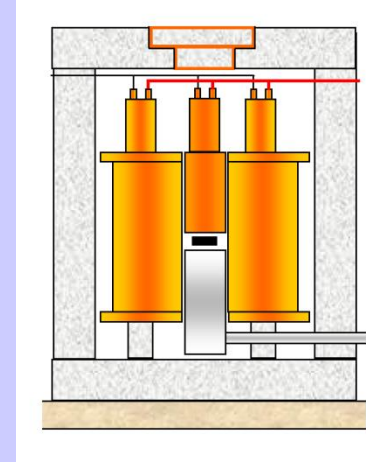
- Standard solutions (^{210}Pb , ^{241}Am , ^{109}Cd , ^{57}Co , ^{113}Sn , ^{137}Cs , ^{54}Mn , ^{65}Zn , ^{139}Ce , ^{60}Co , ^{88}Y)
- Several volume geometries
- Solutions of ^{134}Cs with known activity



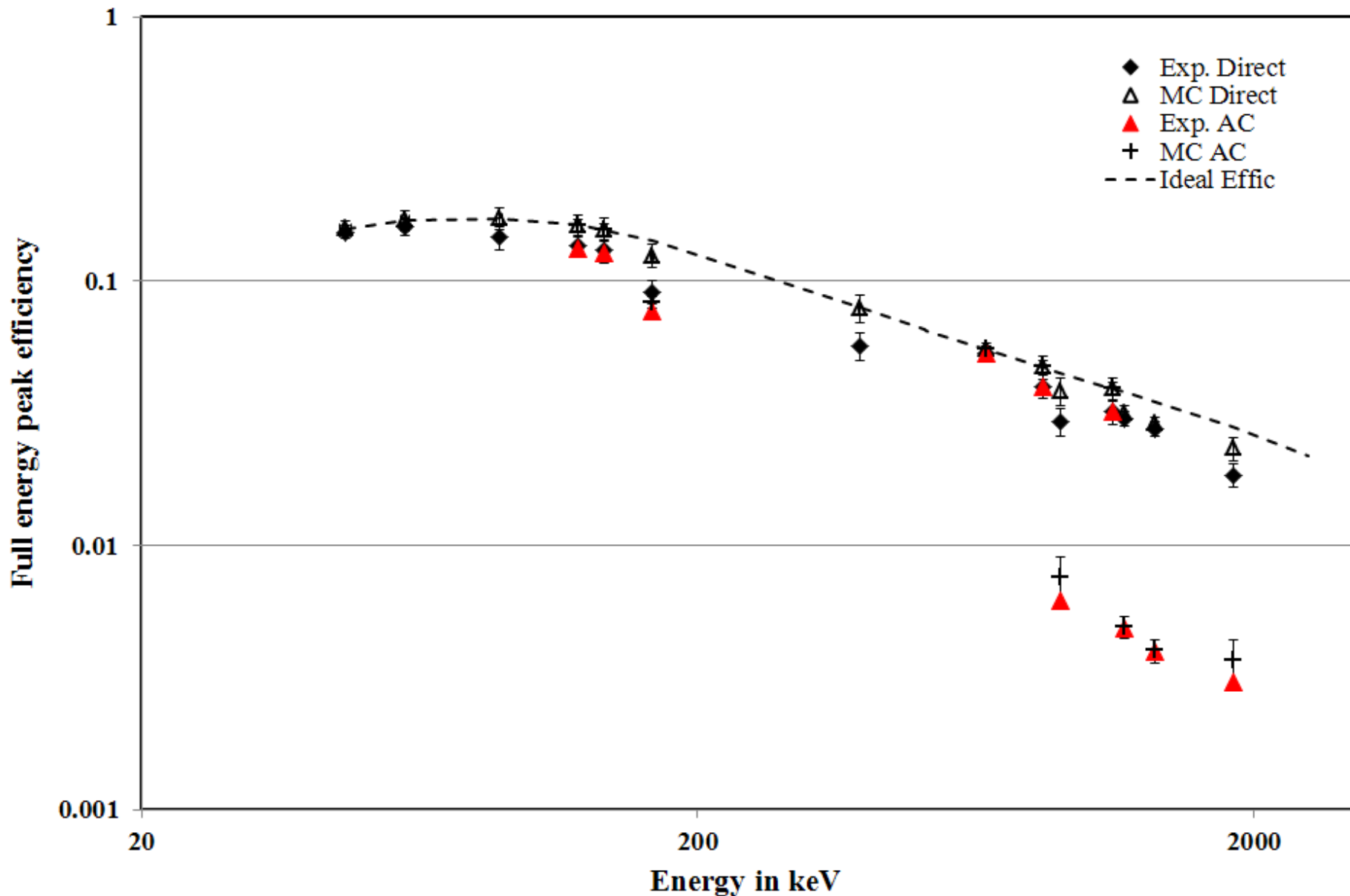
Monte Carlo simulation of the spectrometer

Extension of GESPECOR for this Compton-suppressed spectrometer:

- Implementation of geometry modules
 - Provision for 2 additional layers of absorbers
- Implementation of the veto logic
 - Parameters introduced to control the veto signal:
 - Minimum energy deposited in NaI(Tl) (e.g. discriminators)
 - Efficiency of veto triggering (e.g. time mismatch of signals)
- Fast algorithms, variance reduction techniques
- Coupled with the coincidence summing module

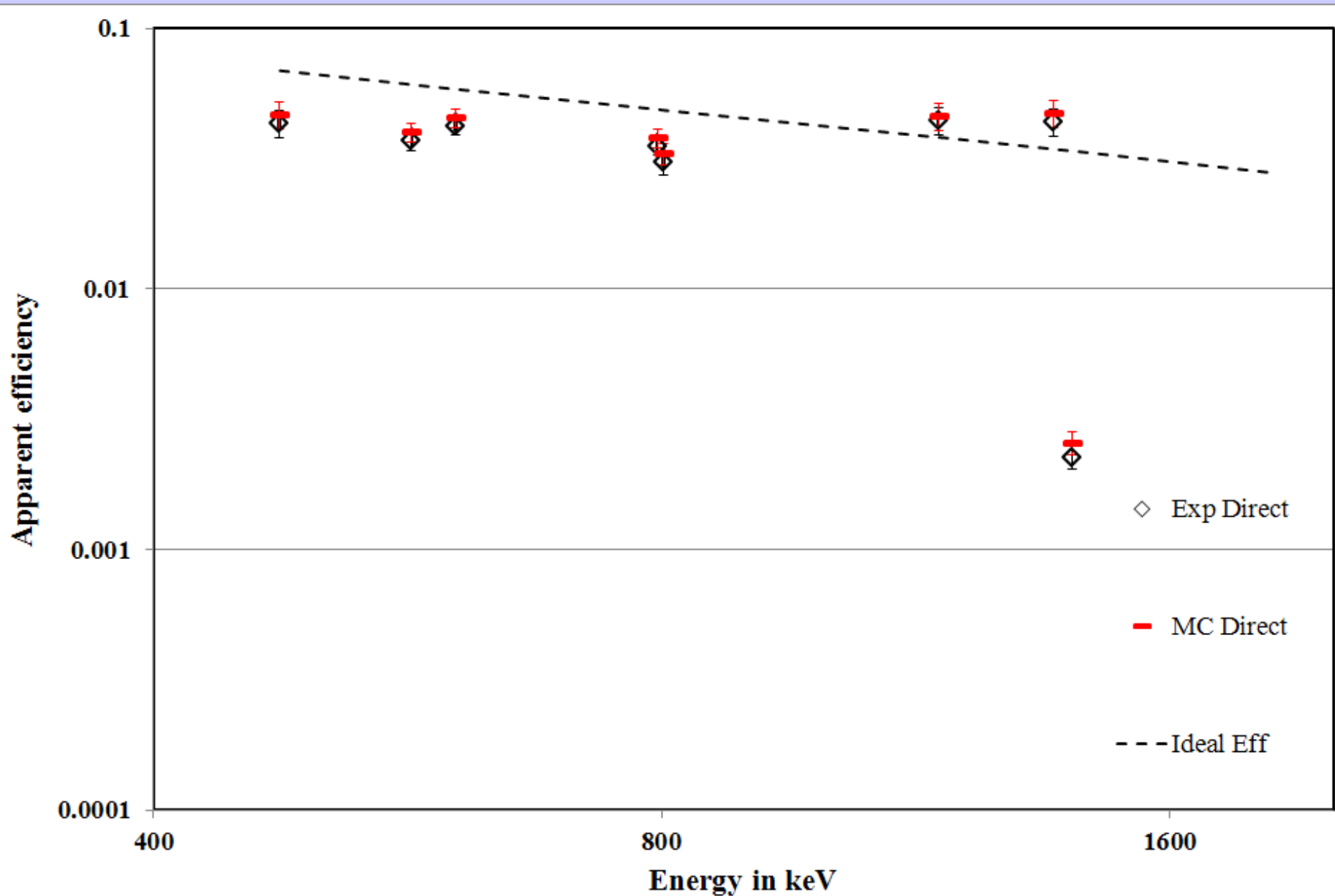


Efficiency calibration for 50 cm³ sample in the Direct and Suppressed Modes



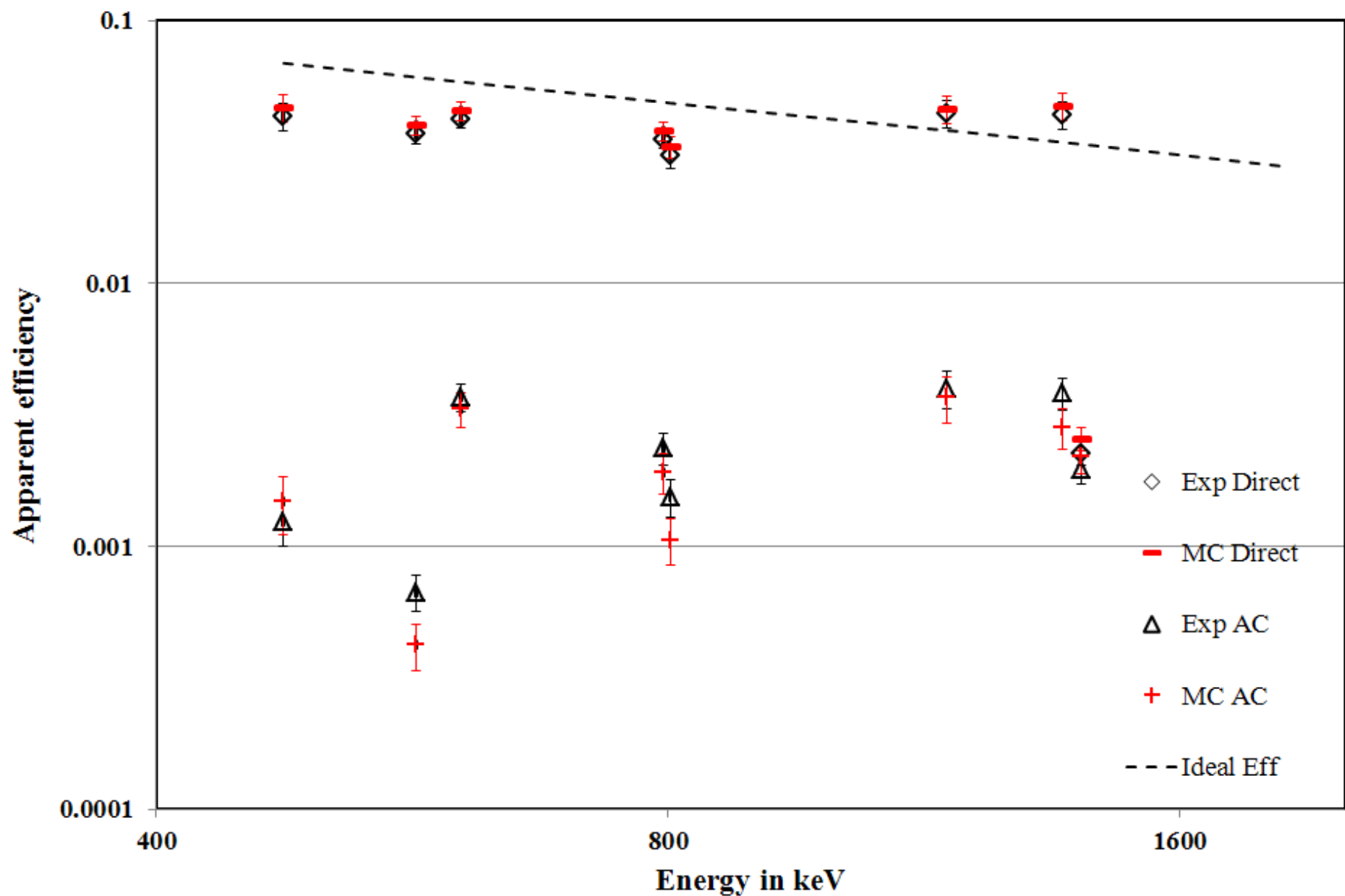
Source: ARI 81 (2013) 76

Efficiency for the peaks of ^{134}Cs for 50 cm³ sample in the Direct Mode



FC values: 0.65 (563, 569), 0.68 (475, 802), 0.78 (604, 796), 1.20 (1167), 1.38(1365)

Efficiency for the peaks of ^{134}Cs for 50 cm³ sample in the Direct and Suppressed Modes

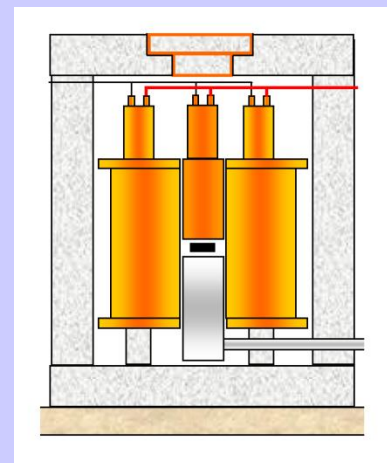
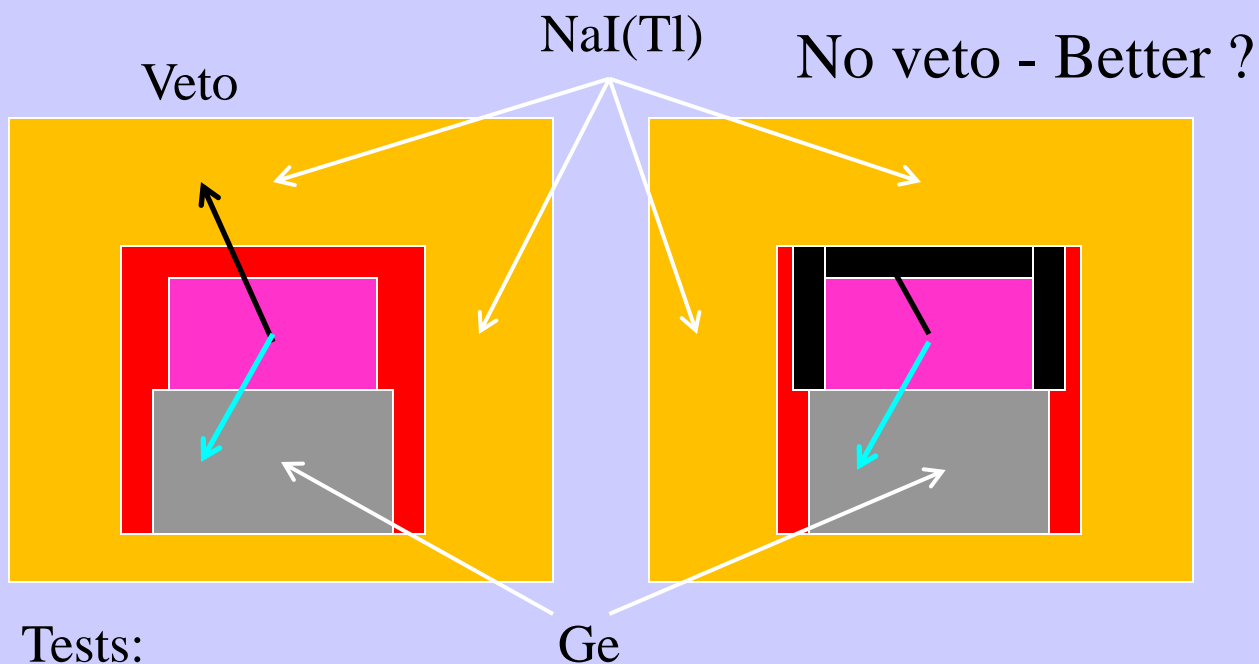


Count Rate Ratio AC/D: 0.03 (475, 802 keV), 0.05 (796), 0.07 (604).

Optimization

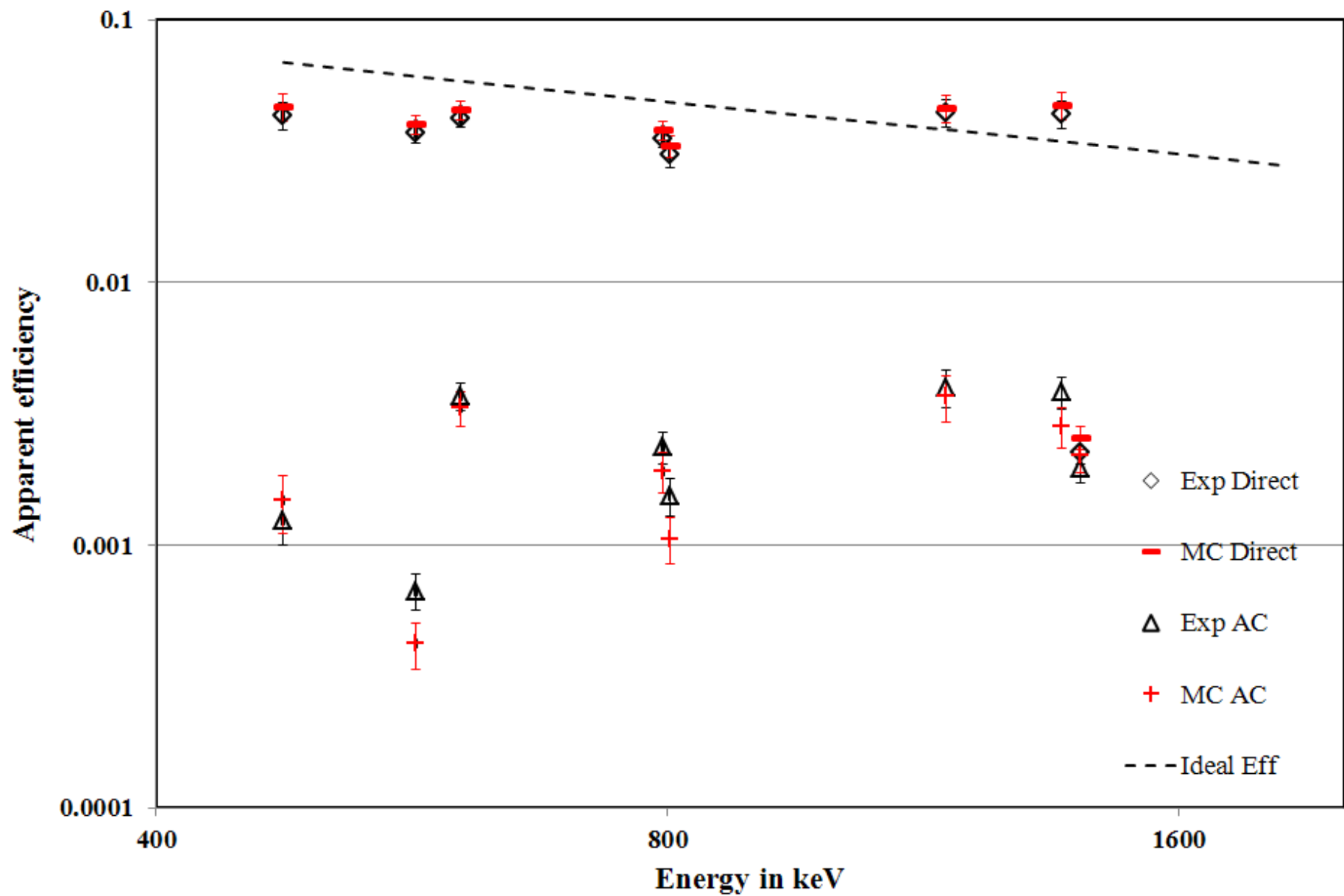
Purpose:

- decrease as much as possible the Compton plateau
 - minimum decrease of the peak count rate
- => compromise

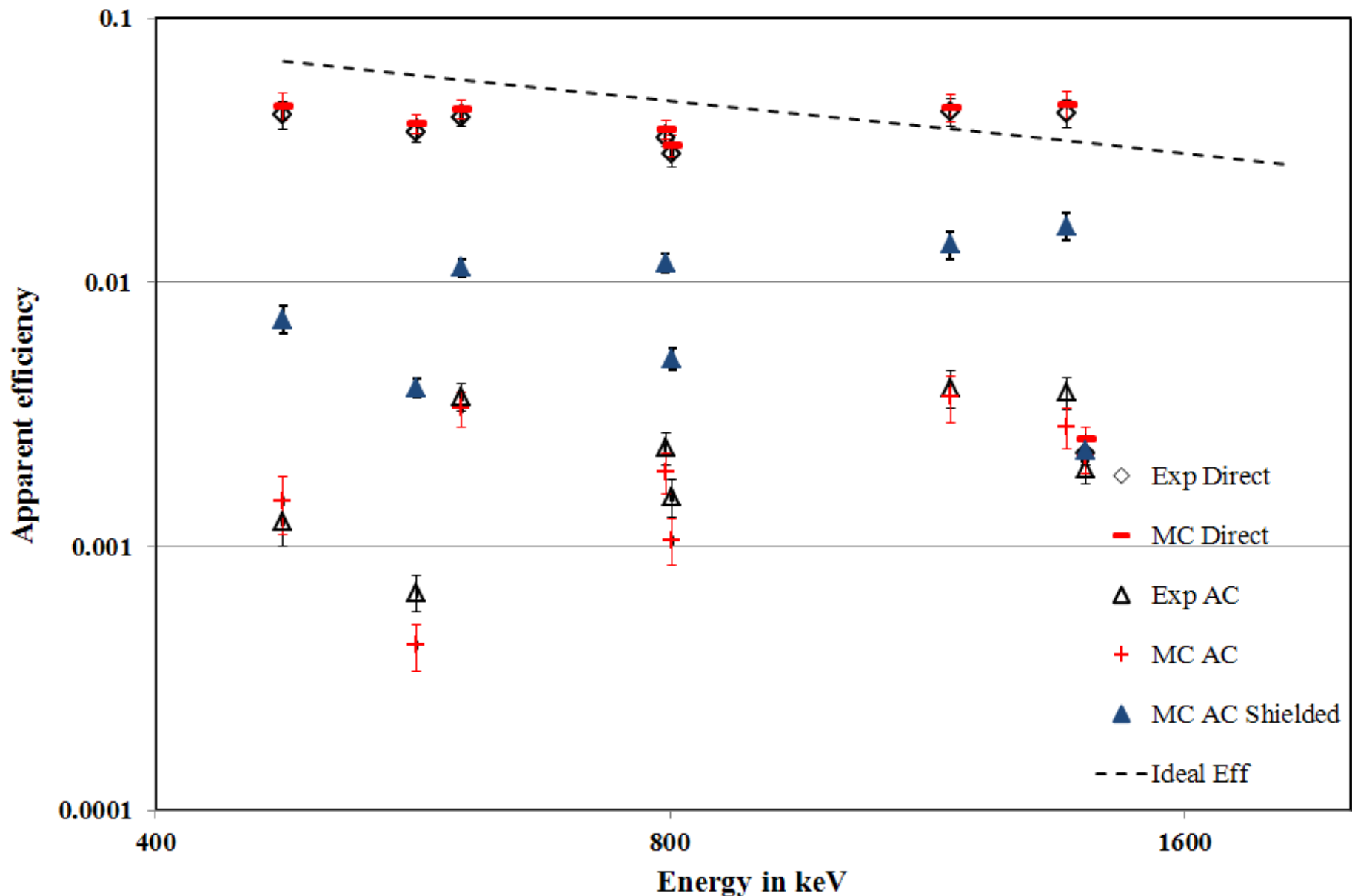


Tests:

- With the top NaI(Tl) decoupled electronically
- With absorbers on side and above the sample (1 mm Cu + 3 mm Pb)



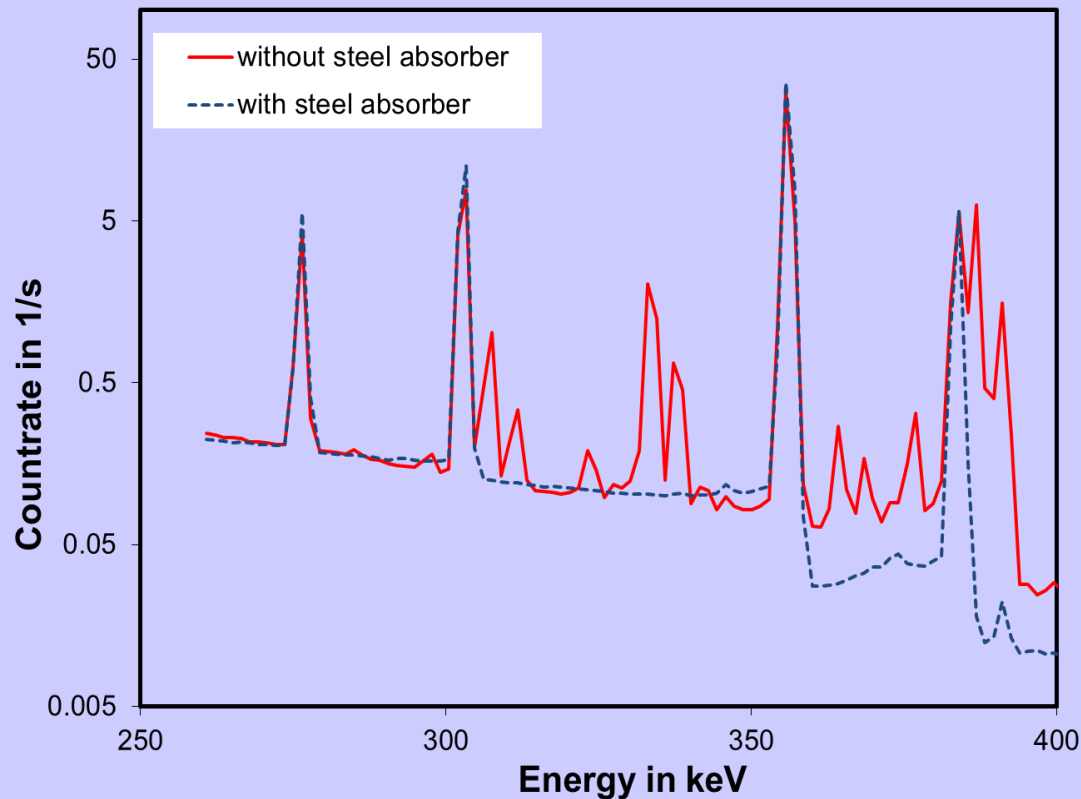
Efficiency for the peaks of ^{134}Cs including the Shielded Geometry in Suppressed Modes



Efficiency improvement by: 4.3 (475 keV), 2.1 (604), 2.7 (796), 2.2 (802) 2.3 (1365)

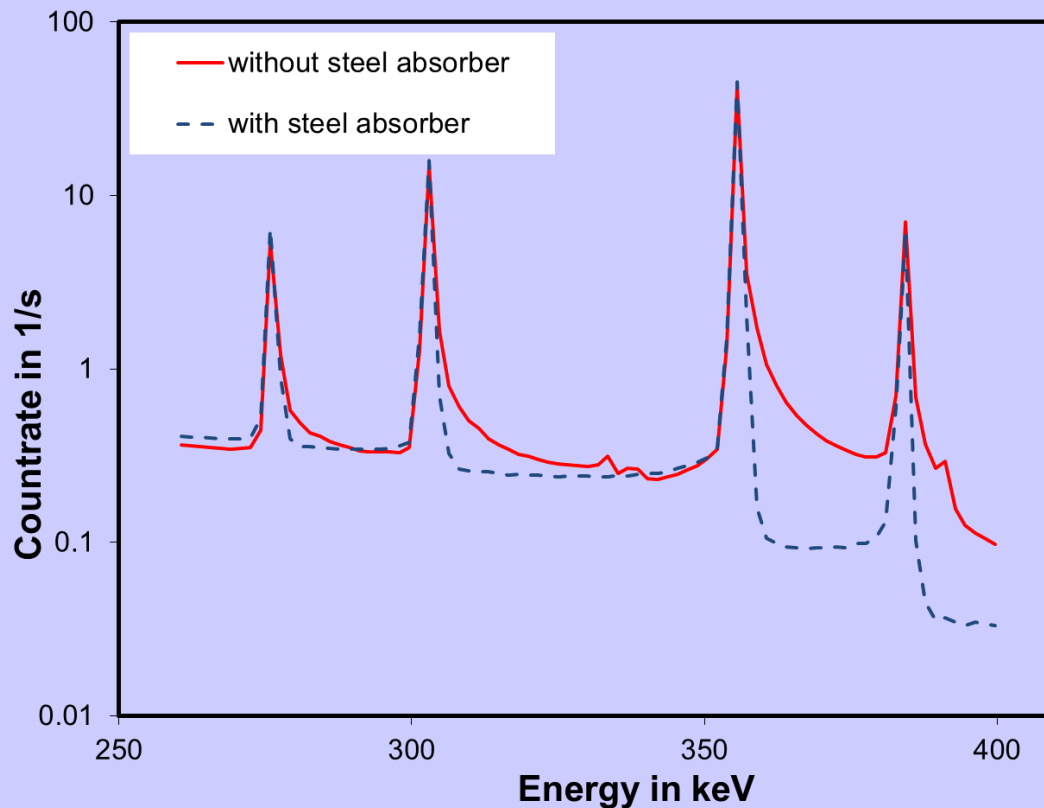
7. Dead layer problem

- Simulations of the total efficiency using the thickness of the dead layer adjusted for reproducing the peak efficiency underestimate the total efficiency
 - P. Dryak et al., ARI 68 (2010) 1451 – experimental values higher by 50%
- Specific shape for peaks affected by coincidence summing with X-rays (p-type detectors) – high energy tail
- Coincidence summing corrections for peaks affected by summing with low energy photons is biased if the thickness of the dead layer appropriate for peak efficiency is used for the computation of the correction factors
 - D. Arnold, O. Sima, ARI 60 (2004) 167
- Peak shape is not reproduced by simulations
 - Stancu et al., Rom. Rep. Phys. 67 (2015) 465



Part of the spectrum of a ^{133}Ba point source measured with an n-type detector, with and without a steel absorber.

- γ photons of ^{133}Ba are emitted simultaneously with X-rays
- With absorber:
 - symmetric peak shape
 - the X-rays do not reach the detector
- Without absorber:
 - significant sum peaks γ +X-rays are observed
 - the shape of the γ peaks is the same as when the absorber is present



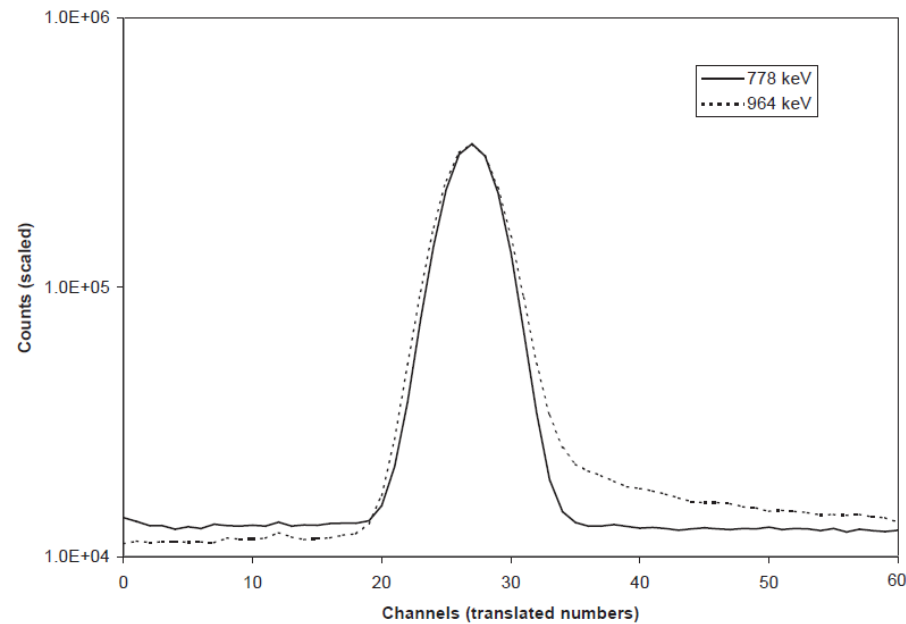
Part of the spectrum of the same ^{133}Ba point source measured with a p-type detector.

- With absorber:
 - symmetric γ peaks shape
 - the X-rays do not reach the detector
 - Without absorber:
 - Tail in the high energy side of γ peaks
 - No sum peaks γ +X-ray observed
- \Rightarrow X-rays deposit only a fraction, not the full energy, in the sensitive volume of the detector, even if the dominant interaction is photoeffect

Comparison of the experimental shape of the peaks of 964 keV and 778 keV of ^{152}Eu

- 964 keV results from EC decay, significant contribution of X-rays to coincidence effects with 964 keV
- 778 keV results from β^- decay, weak contribution of X-rays to coincidence effects with 778 keV

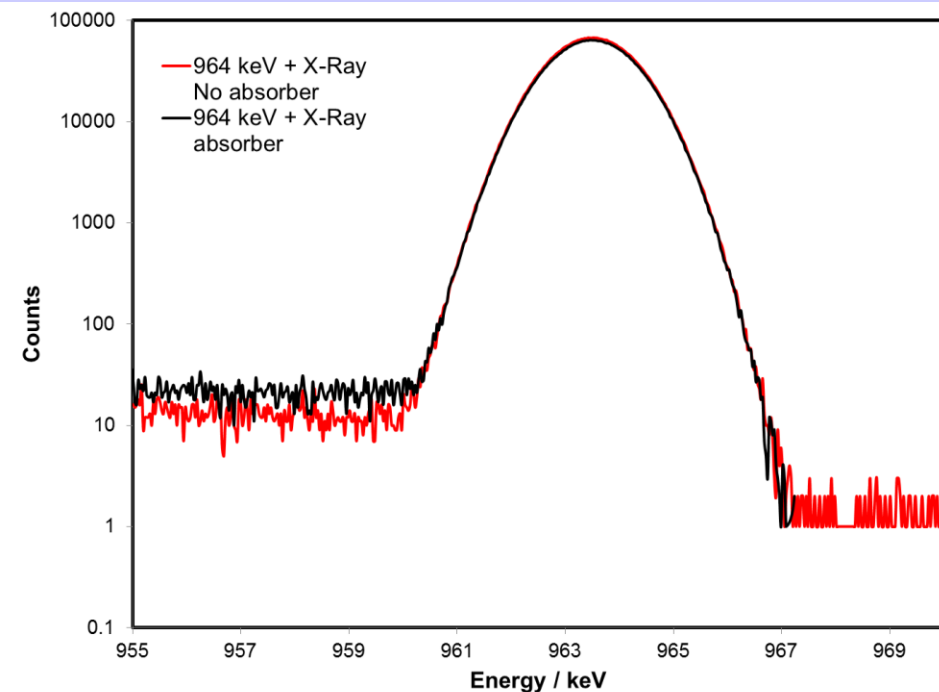
Source: Arnold and Sima, ARI 60 (2004)167



Simulation with PENELOPE of the energy deposited in the sensitive volume of the p-type detector assuming:

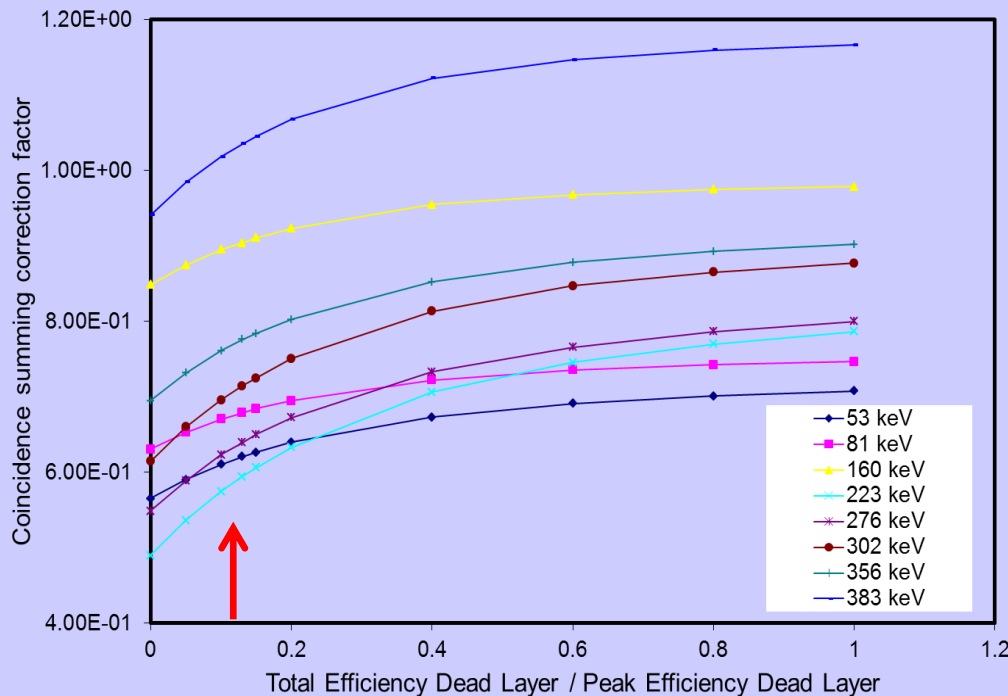
- A sharp dead layer
 - 964 keV γ photon emitted together with an X-ray
1. No absorber
 2. Steel absorber
- => The same peak shape in both cases

Source: Stancu et al., Rom. Rep. Phys. 67 (2015) 465



⇒ The dead layer for a p-type detector has a complex structure

- A region of thickness t_T (dead layer for the total efficiency) – no charge produced in this region is collected – interactions from this region do not contribute to total and to peak efficiency
- A region of thickness t_p (conventional dead layer) – the charge produced in this region is incompletely (or not at all) collected – the interactions from this region do not contribute to peak efficiency
- The interactions from the region with thickness t , $t_T < t < t_p$, contribute to the total efficiency, but not to peak efficiency



Coincidence summing correction factors calculated by GESPECOR as a function of t_T/t_p , where t_p is the conventional dead layer thickness.

- The value of t_T/t_p corresponding to the best match of the simulation to the experimental values is indicated by the arrow (¹³³Ba measurement with the p-type detector)

Source: Stancu et al., RRP 67 (2015) 465

- ⇒ Use of the conventional dead layer for the simulation of the total efficiency and of the coincidence losses from peaks is inappropriate
- ⇒ The effect on coincidence summing can be partly substituted by defining a different thickness of the dead layer $t_T < t_P$ for the evaluation of coincidence losses

- Incomplete charge collection from domains located in the conventional dead layer is not included in routine Monte Carlo simulations of the germanium detectors

- Peak shape is not correctly reproduced for peaks affected by coincidences with X-rays

- A consistent description requires inclusion of the charge collection process in the simulation

8. Conclusions

Monte Carlo simulation is a very good tool (sometimes the only tool) for solving many problems of interest in gamma ray spectrometry, including special and difficult problems

Future developments:

- Inclusion of charge movement in the electric field and signal processing in simulation.
- Better detector models
 - Standardization of detector dimensions and of detector performance by the detector manufacturers
- Improved uncertainty estimation